Micromechanics of Solid Foams with Open Cells

SAND2010-3338C

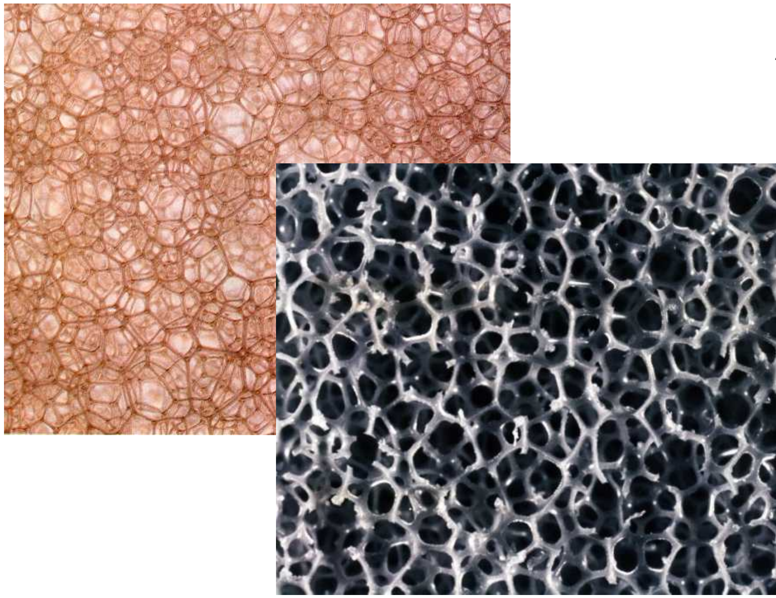

Andy Kraynik, Sandia National Labs

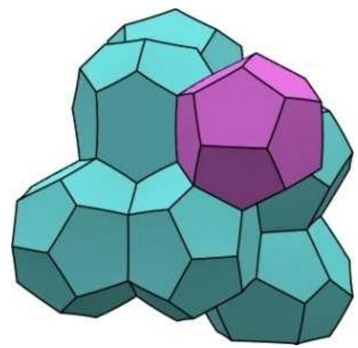

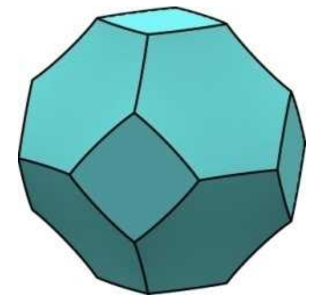

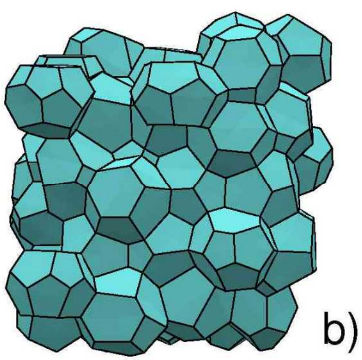

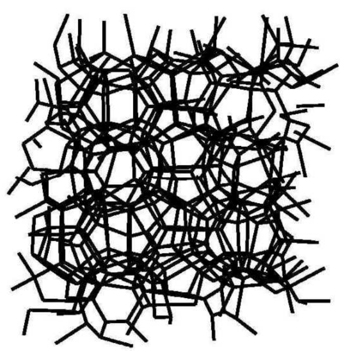

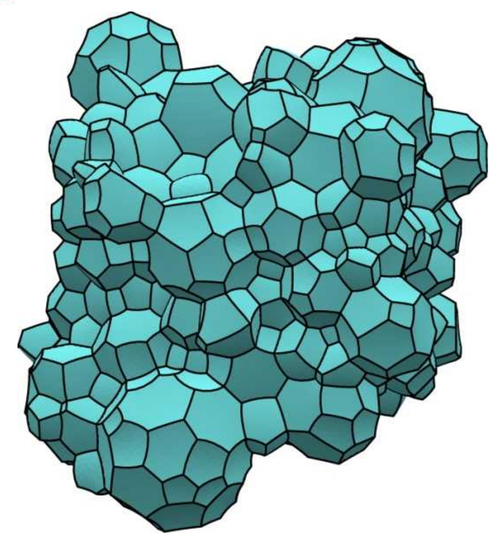

Sandia is a multiprogram laboratory operated by Sandia Corporation, a Lockheed Martin Company, for the U.S. Department of Energy's National Nuclear Security Administration under contract #DE-AC04-94AL85000.

Denser liquid foams are softer – G decreases with ρ

Liquid Foams

$G_f \sim \sigma / R_{32}$

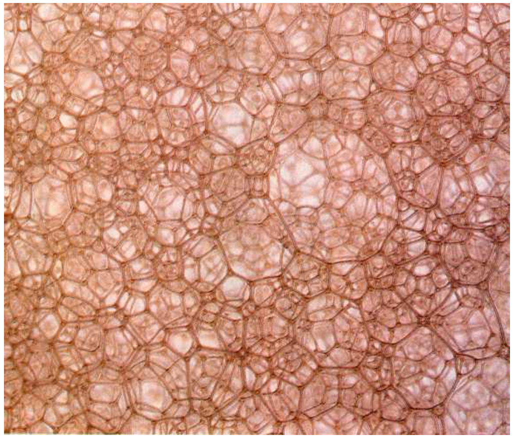

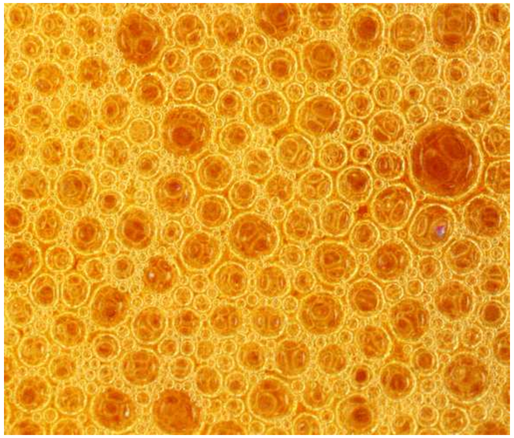

Denser solid foams are stiffer – G increases with ρ

Solid Foams

$G_f \sim E\,\phi^2$

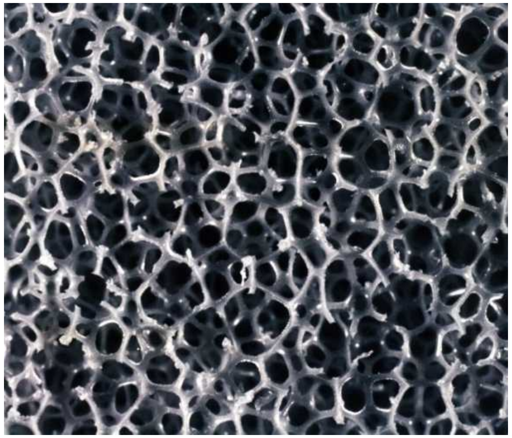

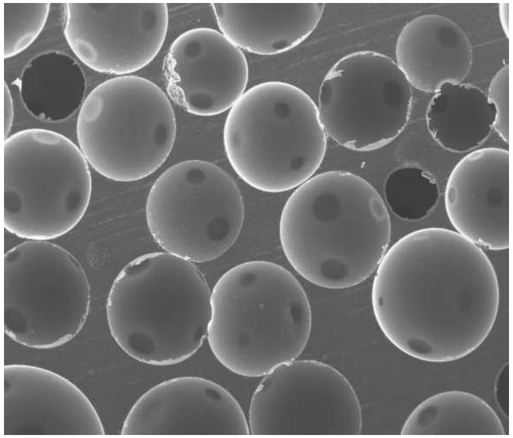

Predicting structure-property-processing relationships involves the fluid mechanics and solid mechanics of foams

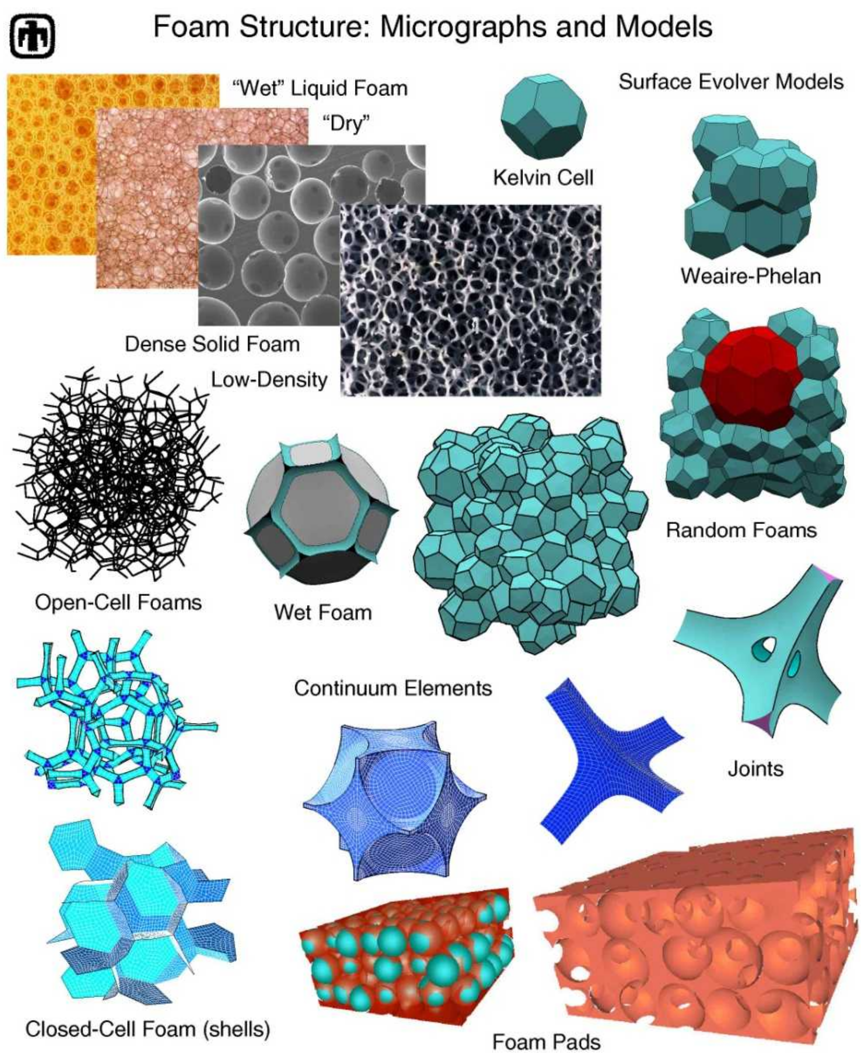

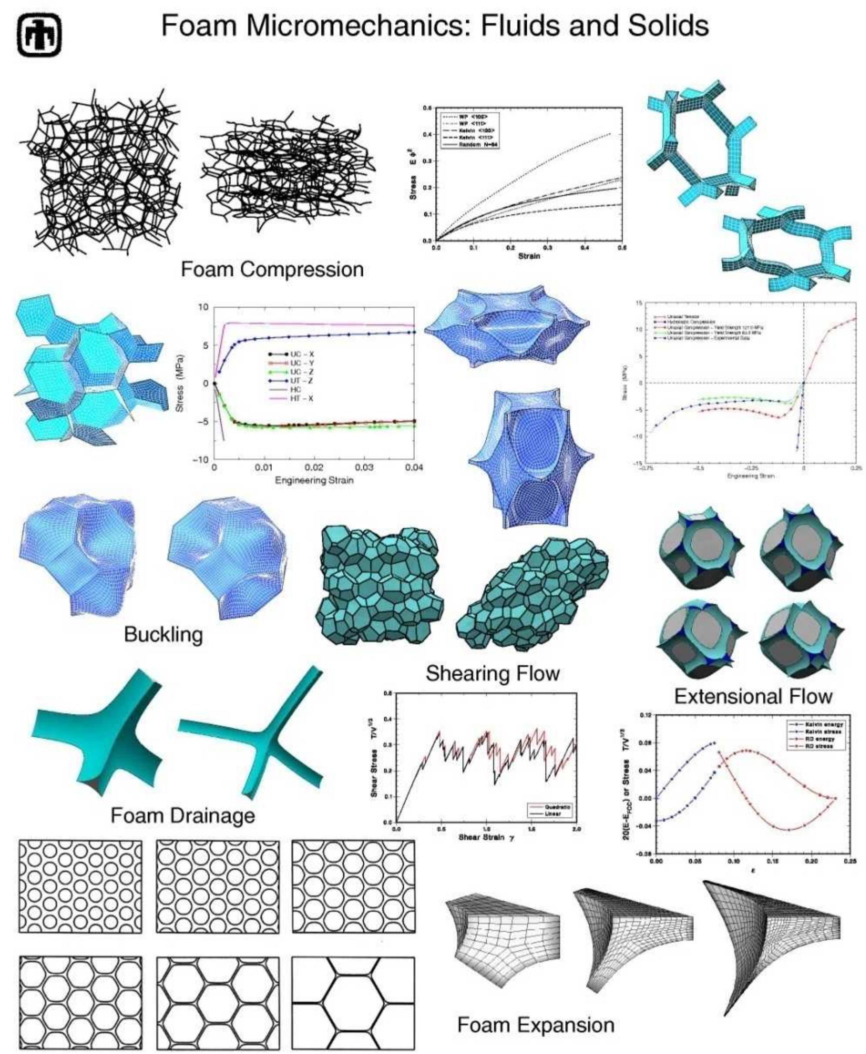

The cell structure of low-density foams can be viewed as polyhedra packed to fill space

Liquid Foam

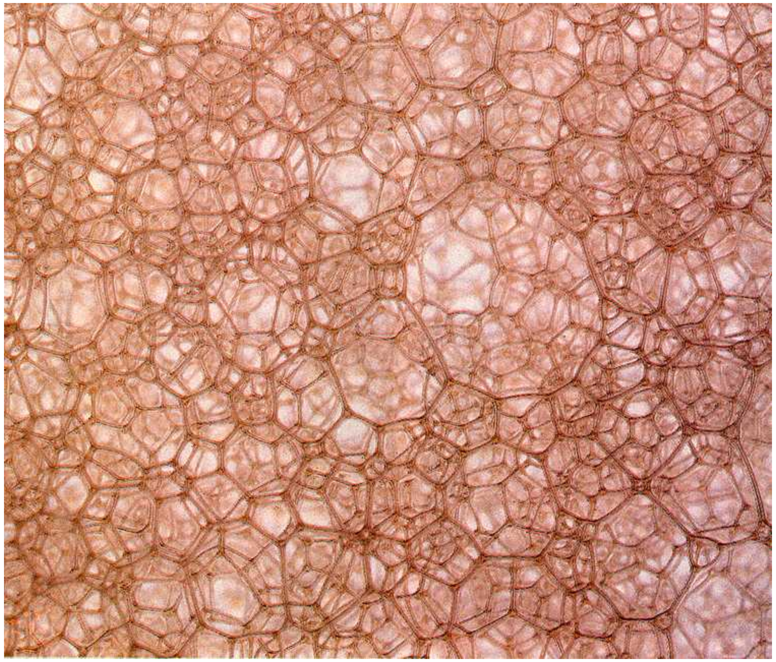

Dry Soap Froth

Solid Foam

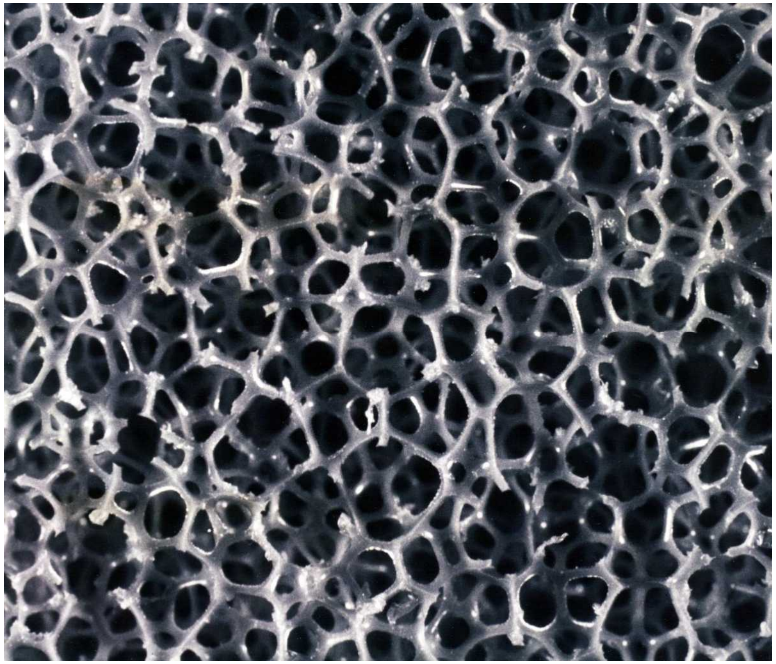

Low-Density Open-Cell Foam
e.g., Flexible Polyurethane Foam

Confocal microscopy of Plateau borders in emulsions

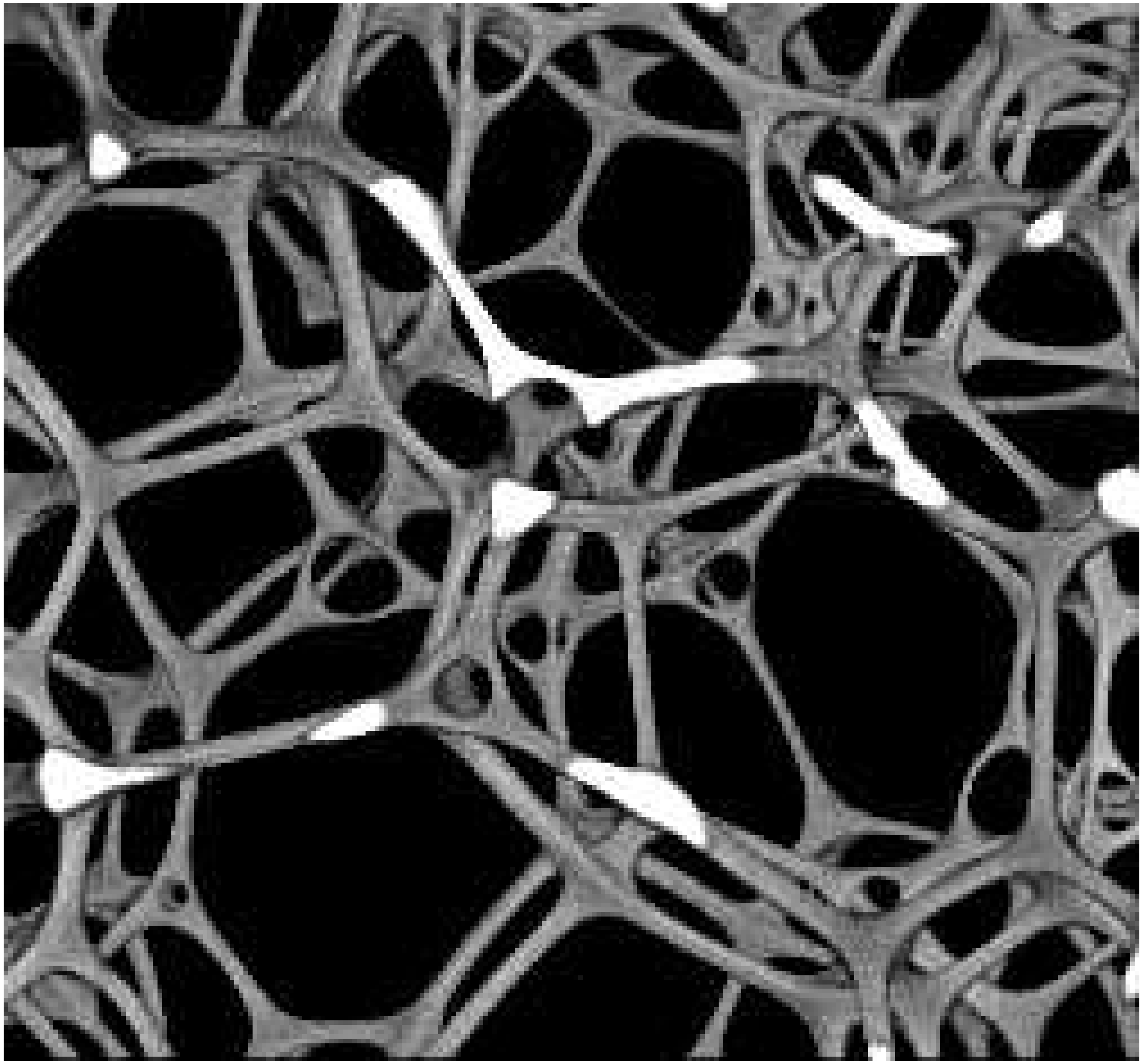

Eric Weeks, Physics, Emory University and Doug Wise, Physics, Harvard University

Polyurethane foam skeleton from image analysis of MRI and XMT data

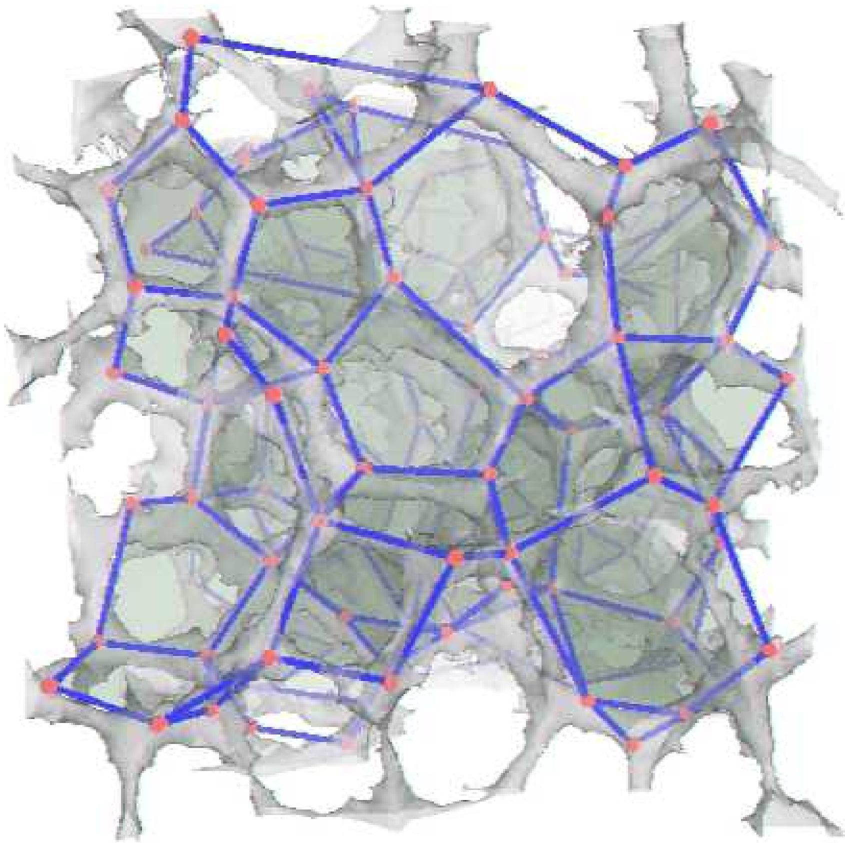

Matt Montminy, PhD thesis, U Minnesota (2001)

Montminy, Tannenbaum & Macosko,
The 3D structure of real polymer foams,
J. Coll. Int. Sci. **280** 202-211 (2004).

Strut length distribution

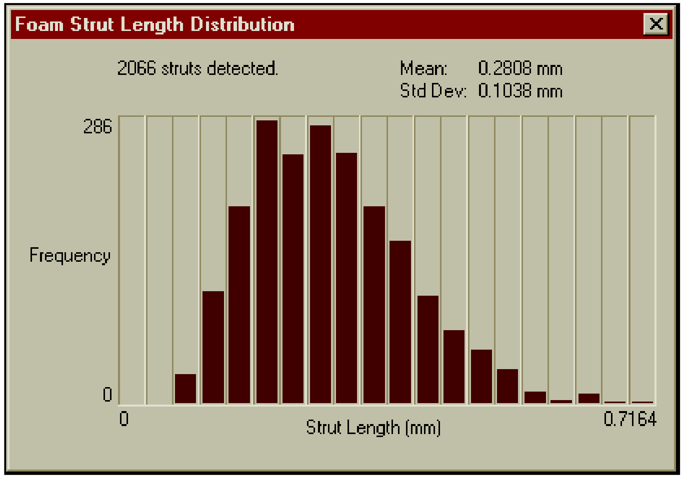

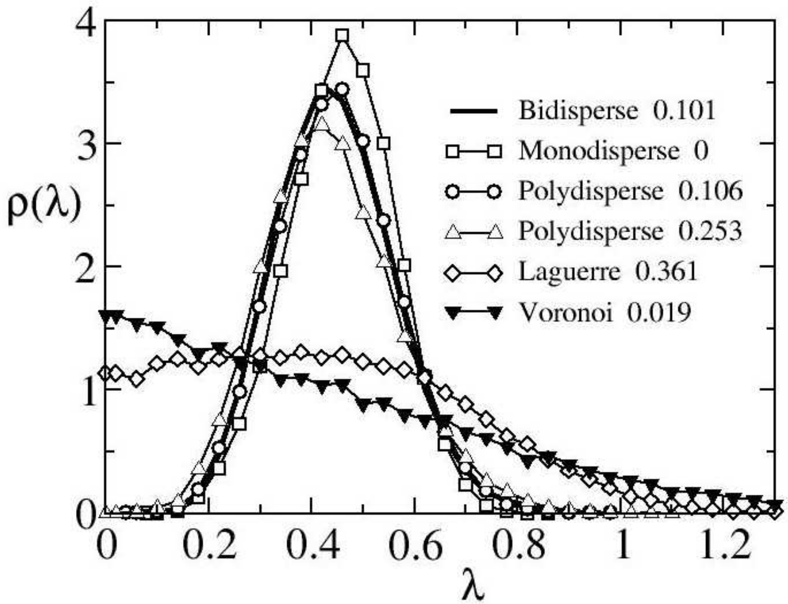

Modeling low-density open-cell foams

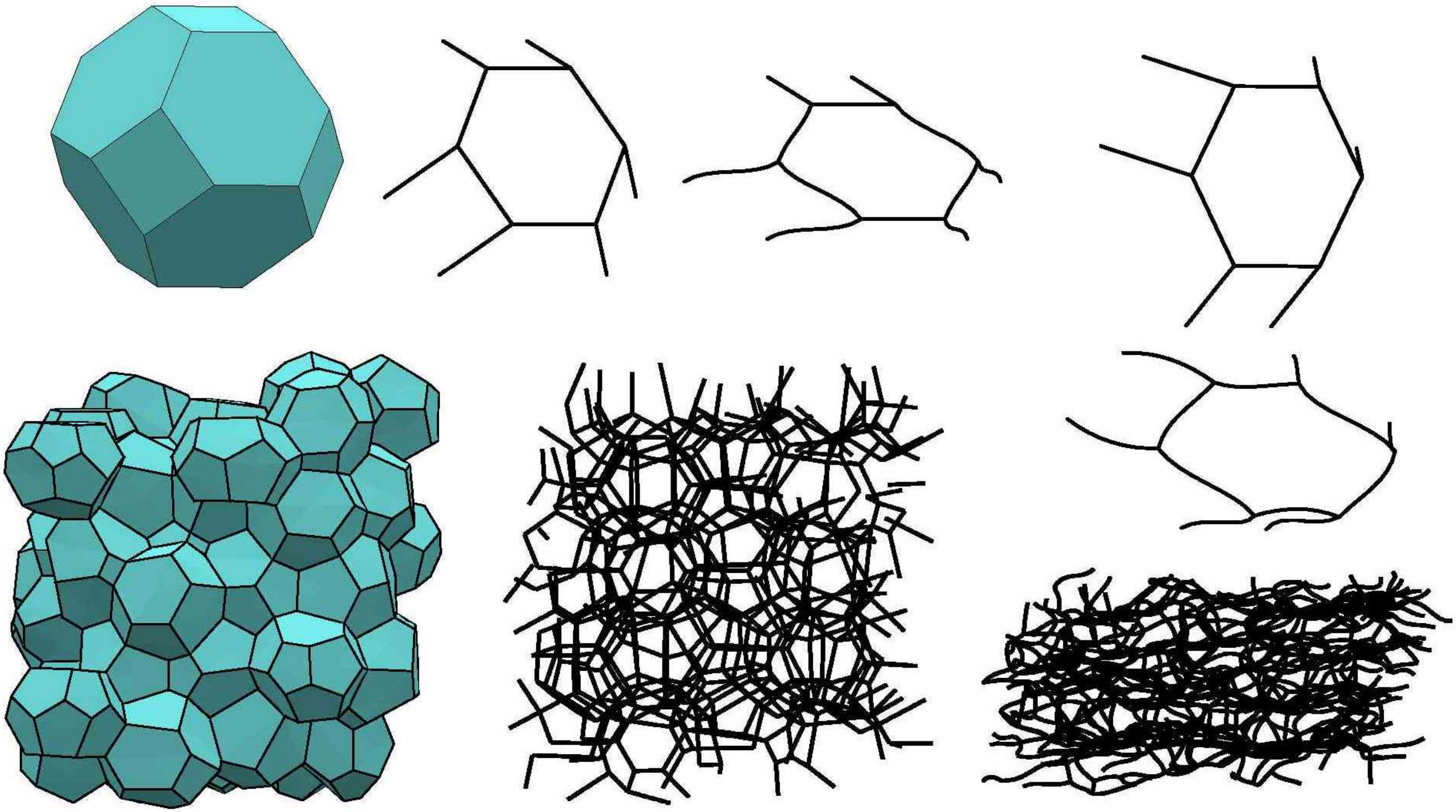

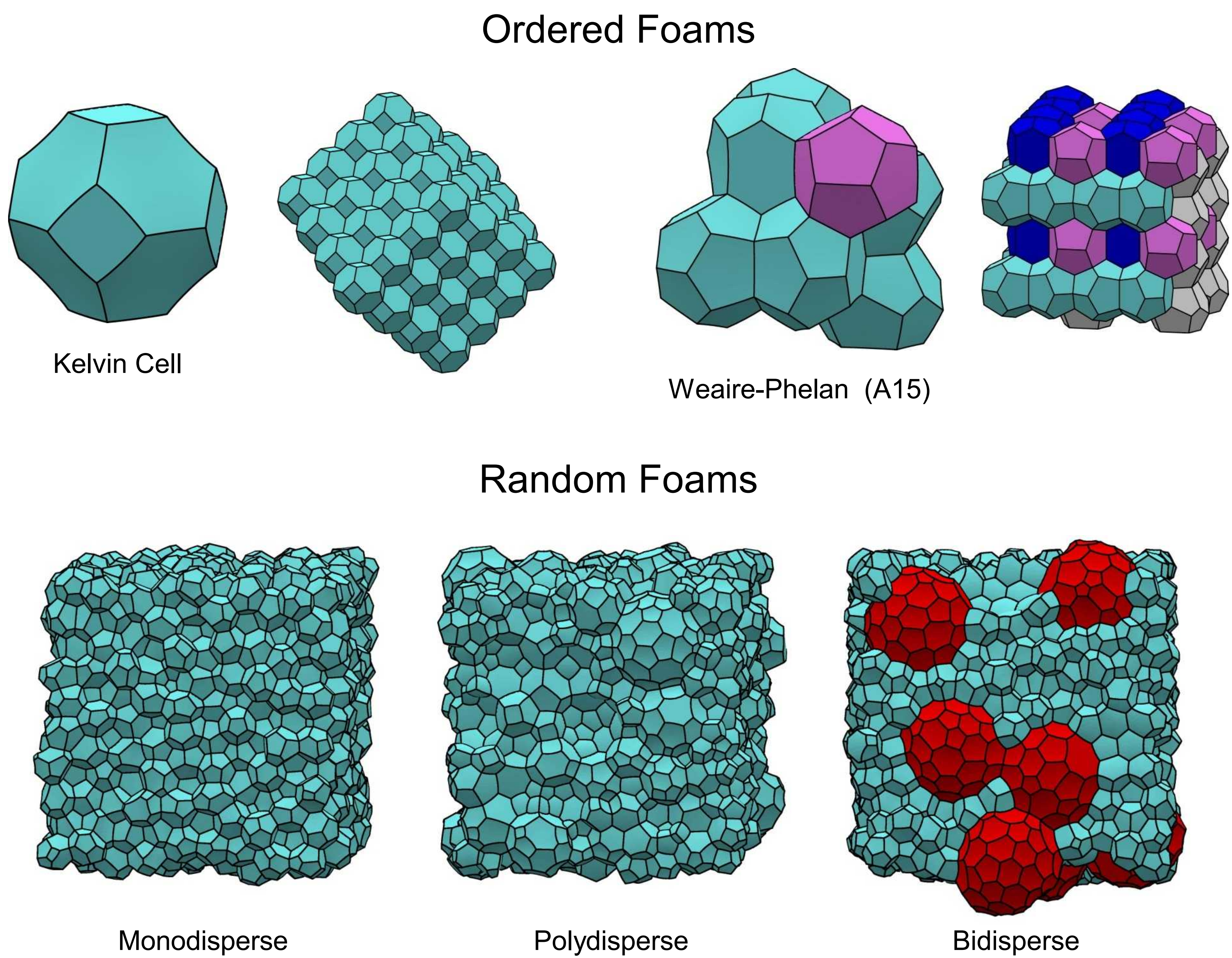
Ordered Foams
Kelvin Cell
Weaire-Phelan (A15)
Random Foams
Monodisperse
Polydisperse
Bidisperse

Gibson-Ashby Correlation for Open-Cell Foams

$$E_f = E\,\phi^2$$

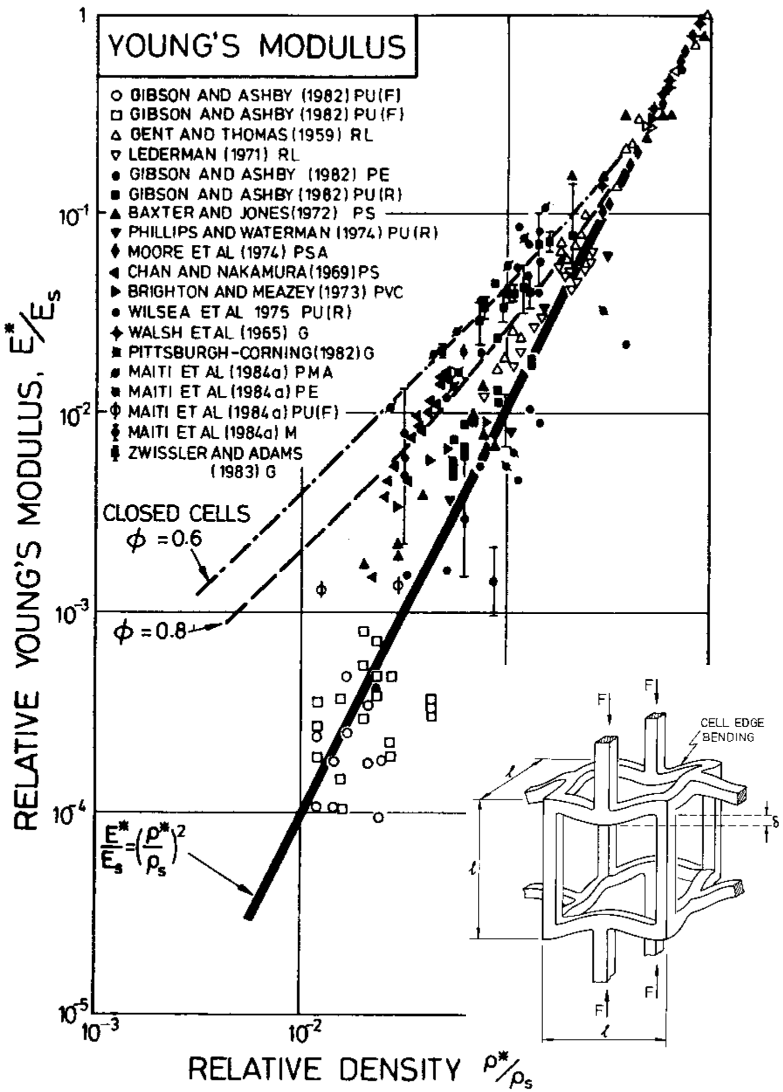

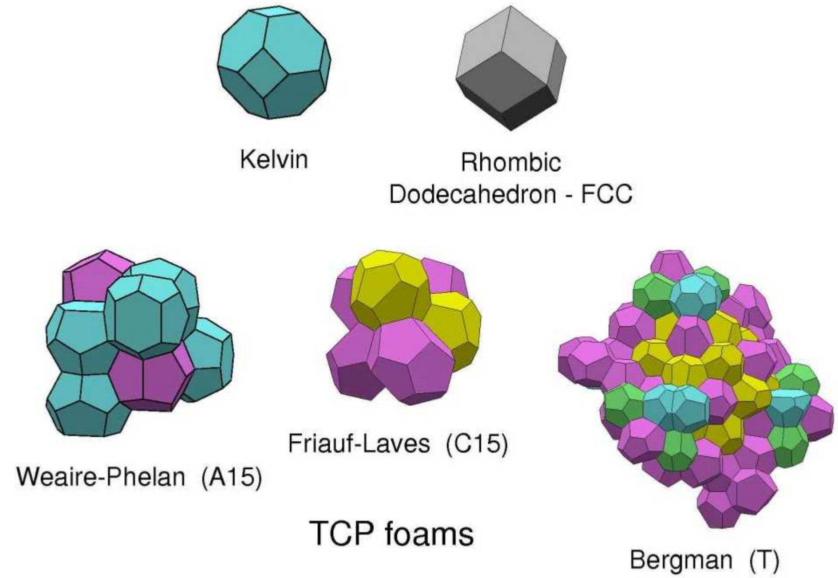

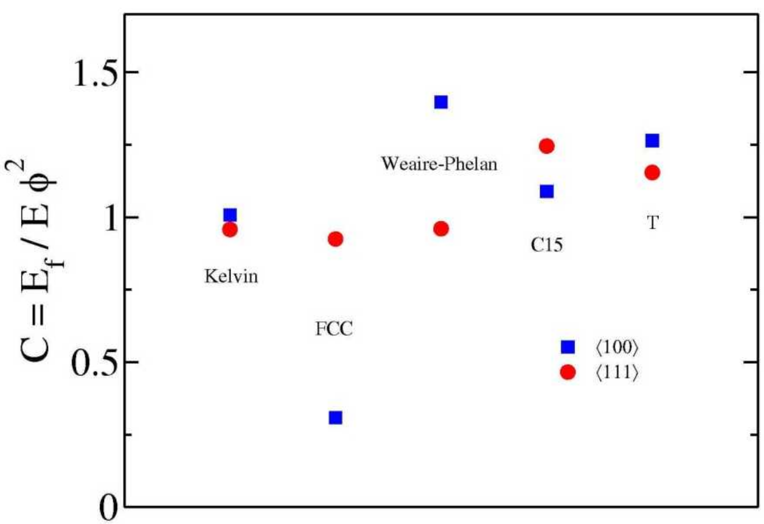

Modeling low-density open-cell foams with random structure

Soap Froth

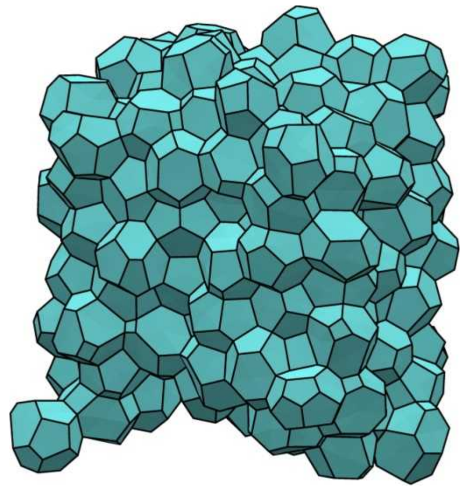

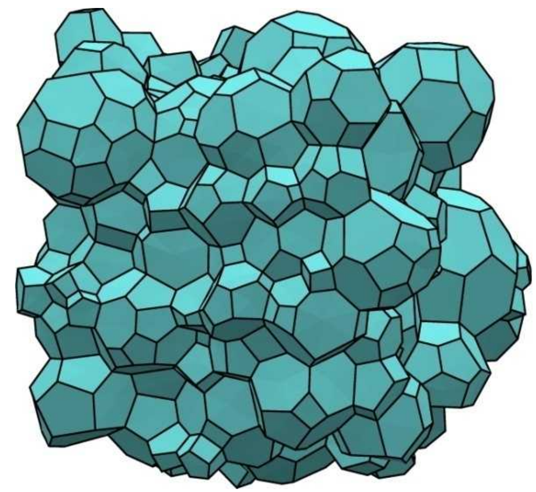

monodisperse

polydisperse

Finite Element Model
Beam Elements

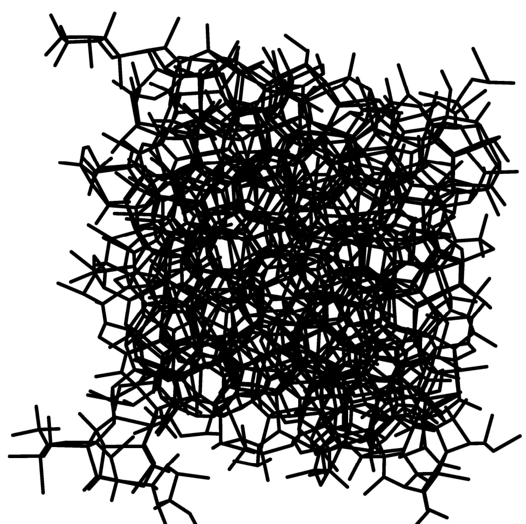

The edge-length distribution of Voronoi structures is very different from foams

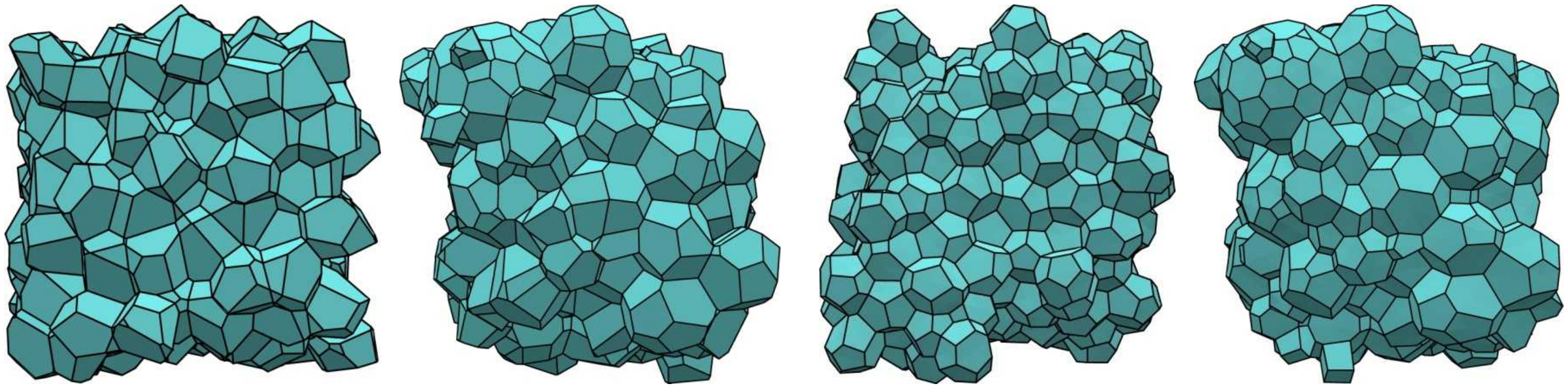

Voronoi Laguerre monodisperse foam polydisperse foam

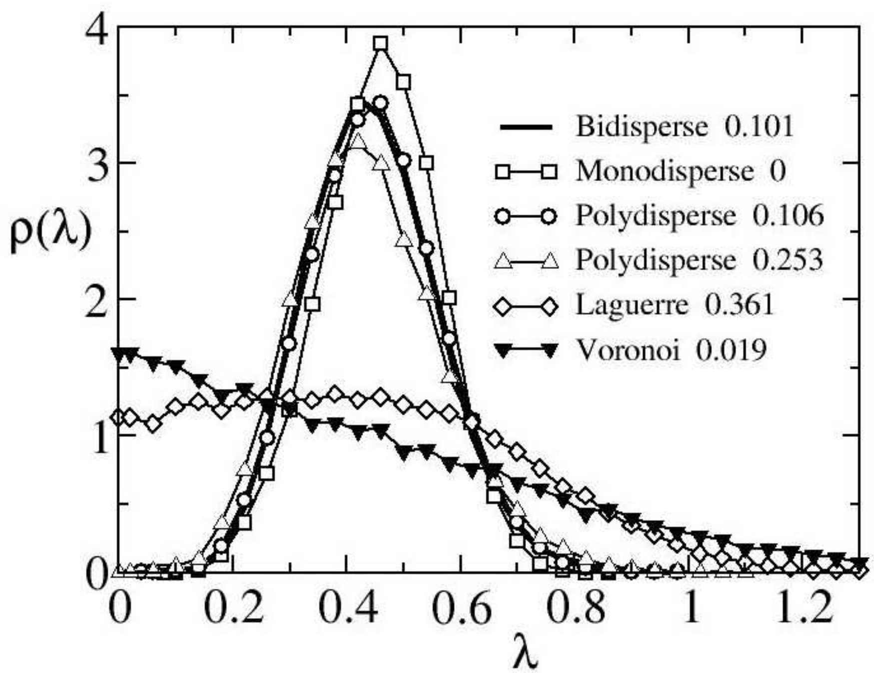

Young's modulus of low-density open-cell foams

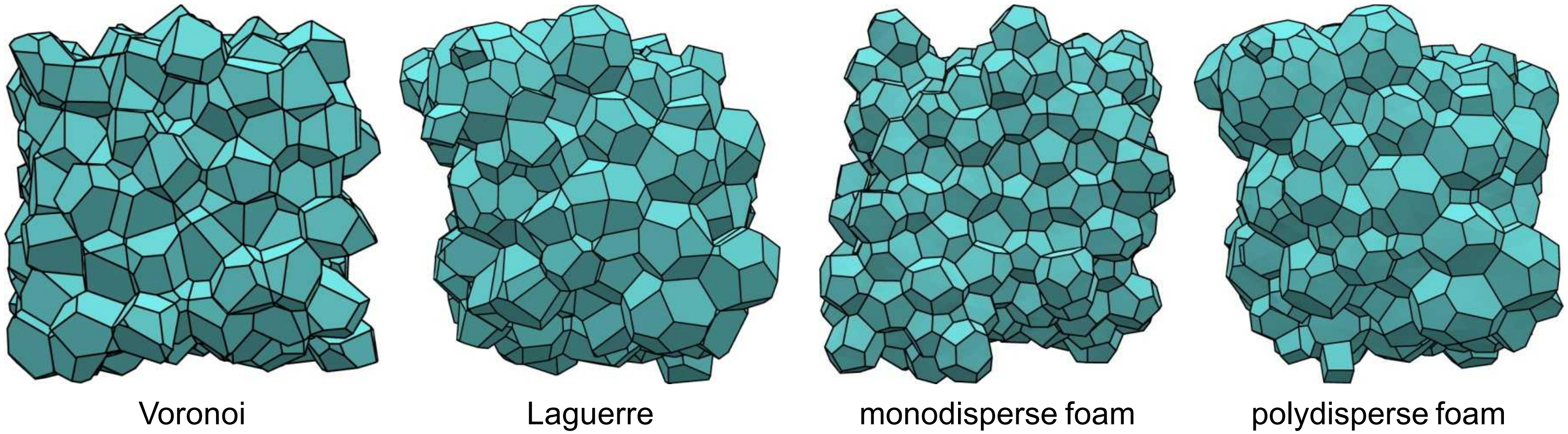

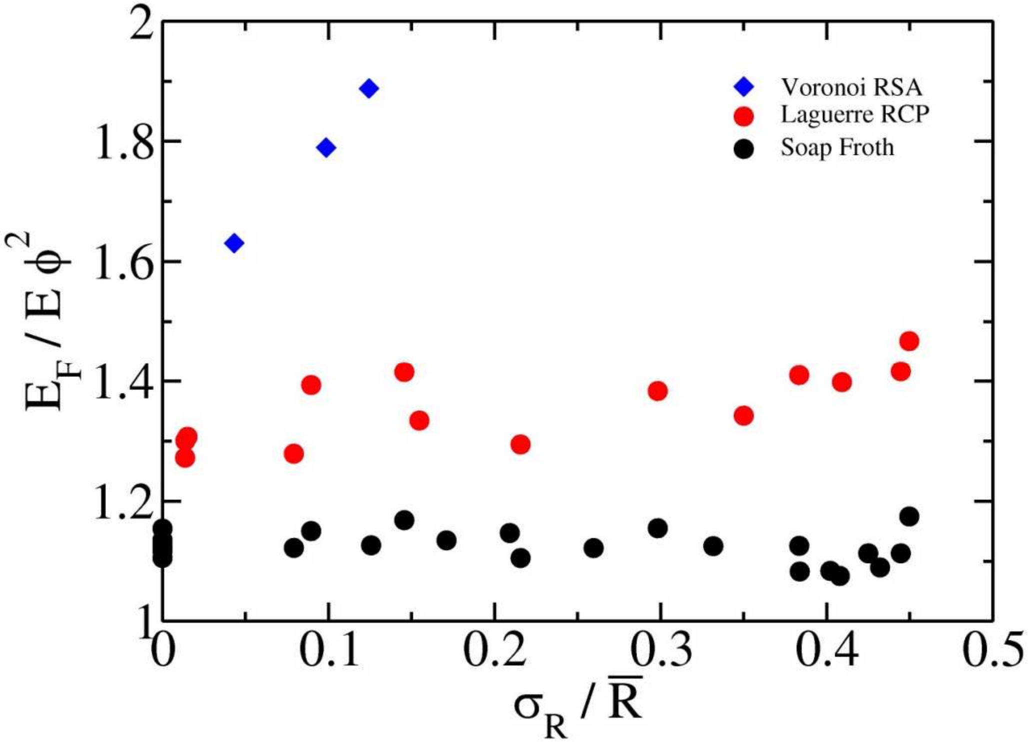

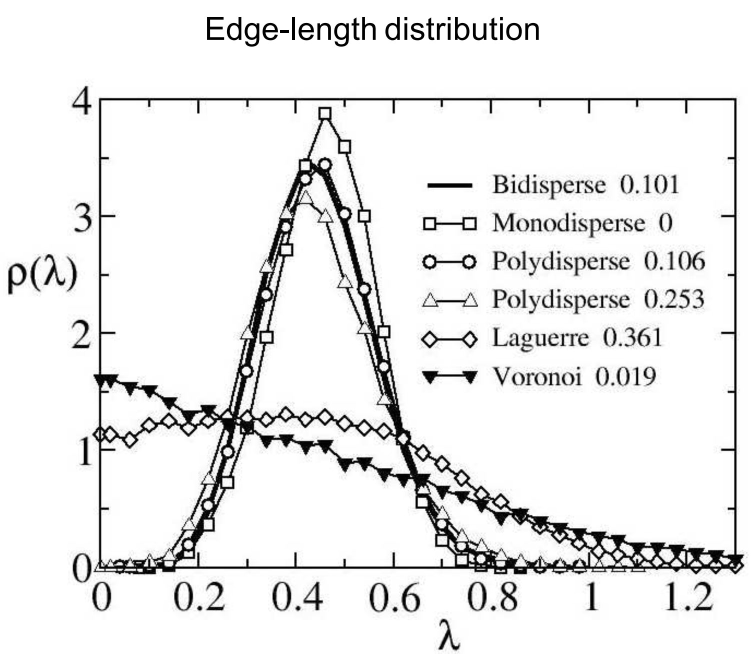

Simulation of Uniaxial Compression

Animation by Mike Neilsen

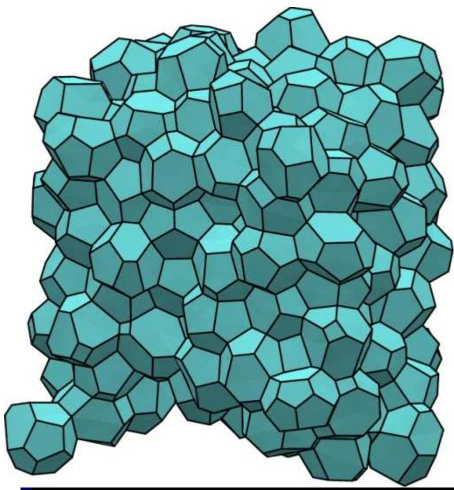

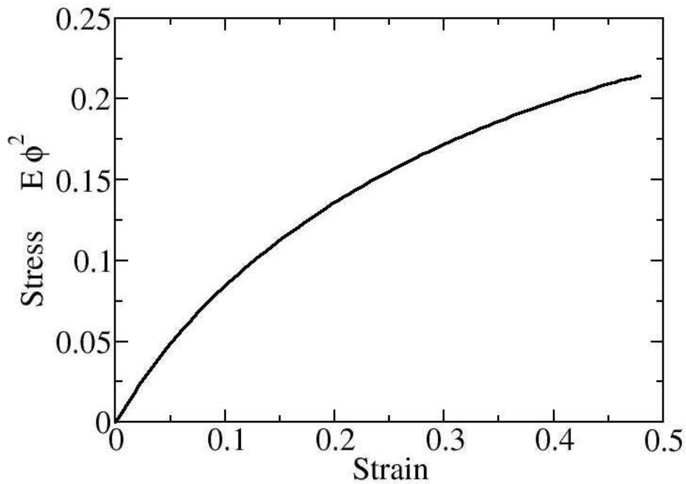

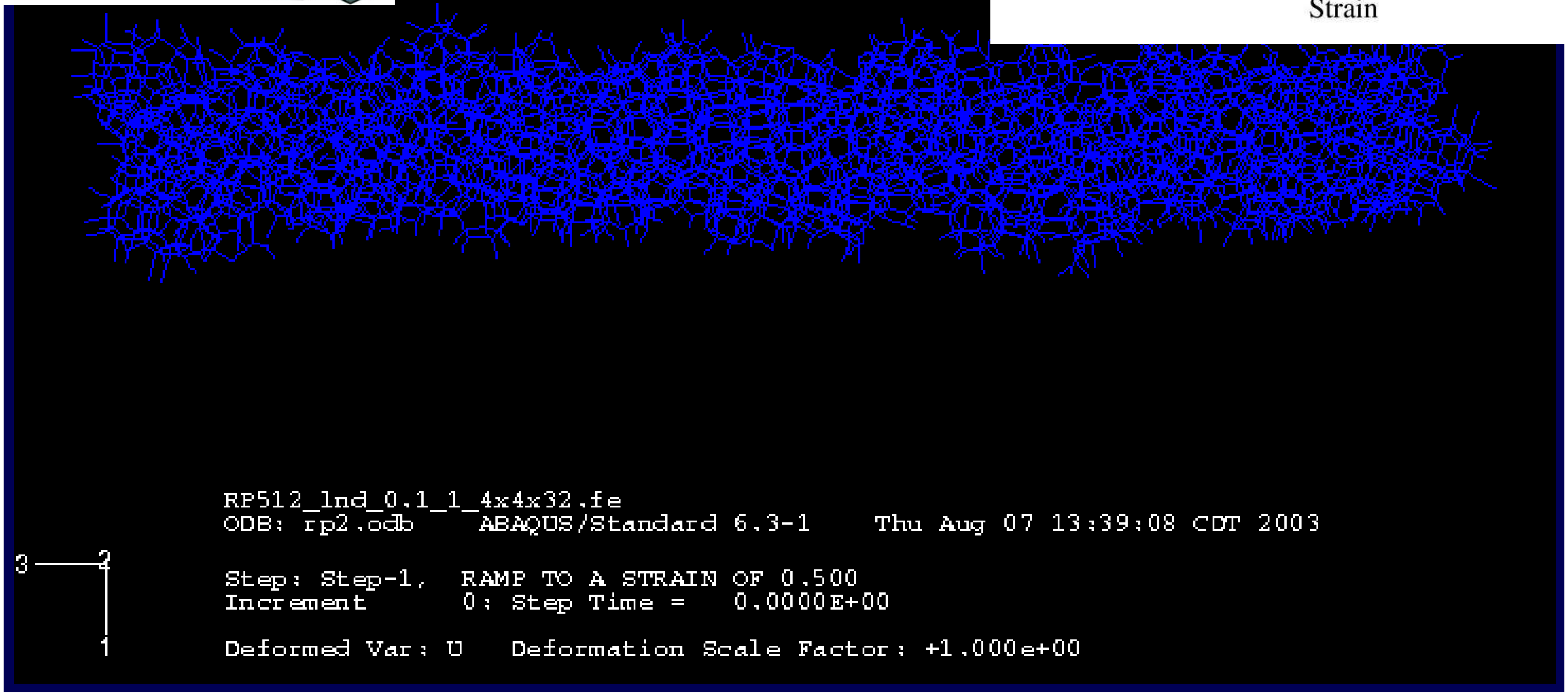

Uniaxial compression of low-density open-cell foams

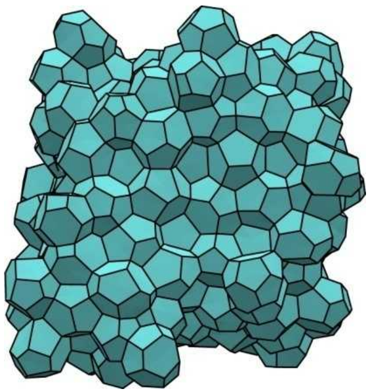

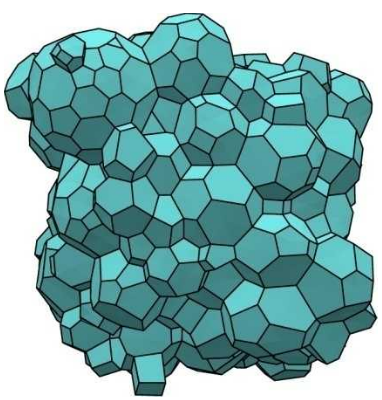

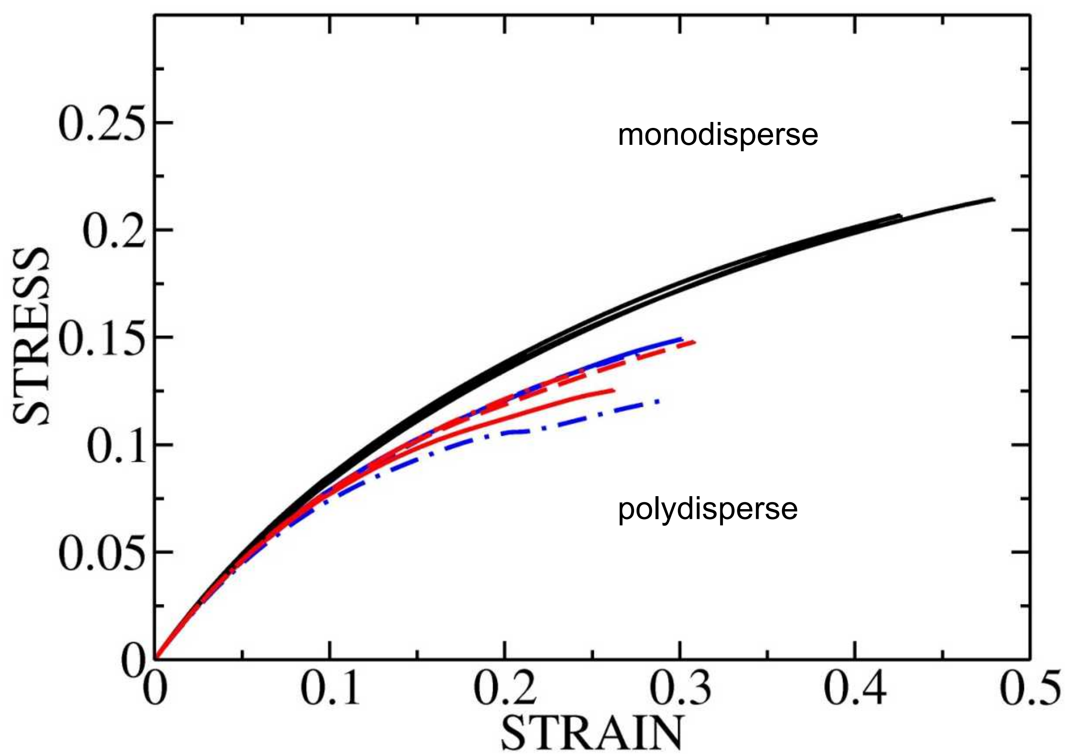

Plateau Borders in a Wet Kelvin Foam

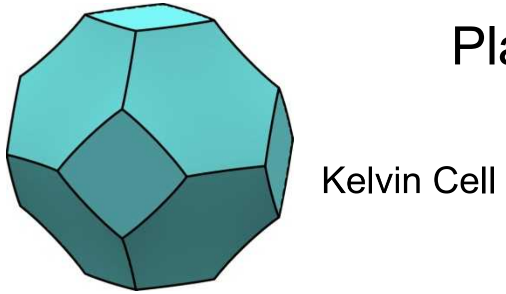

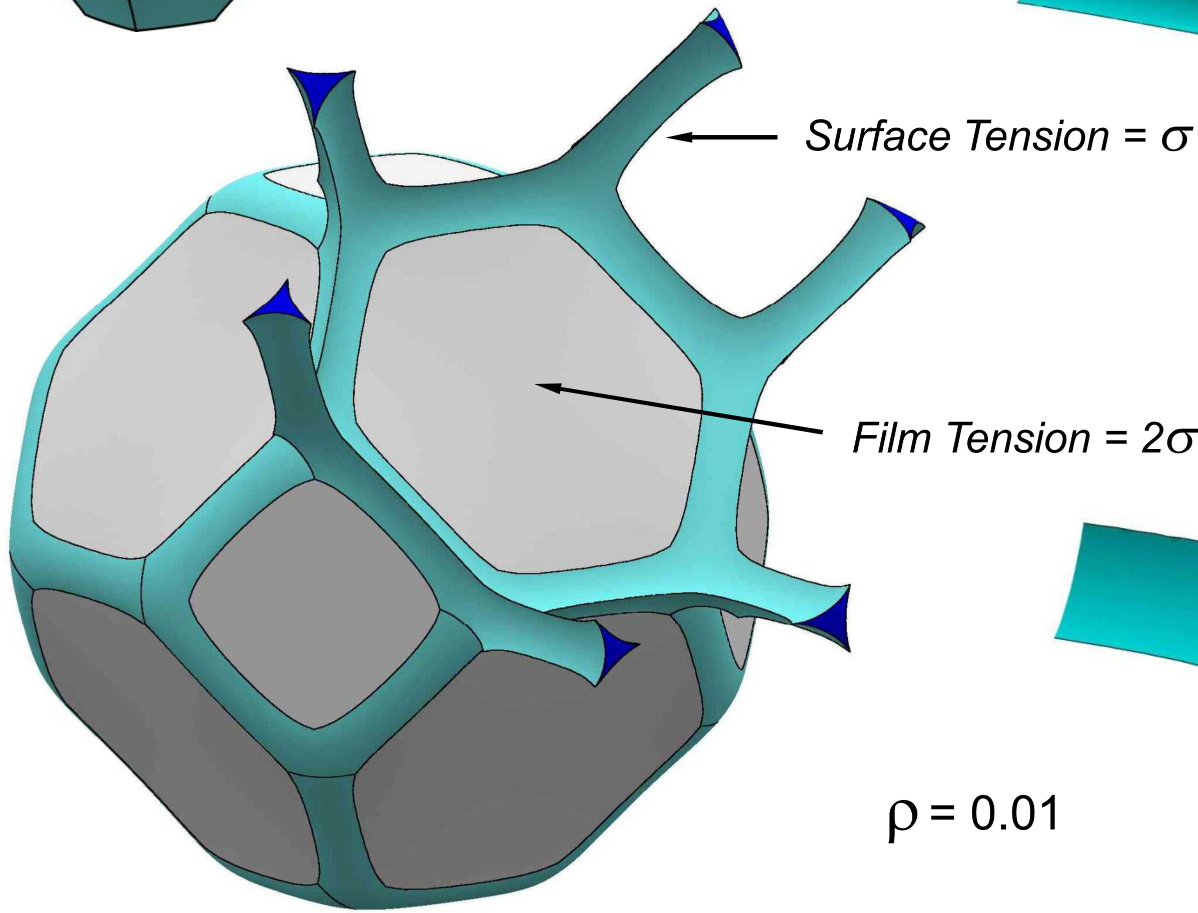

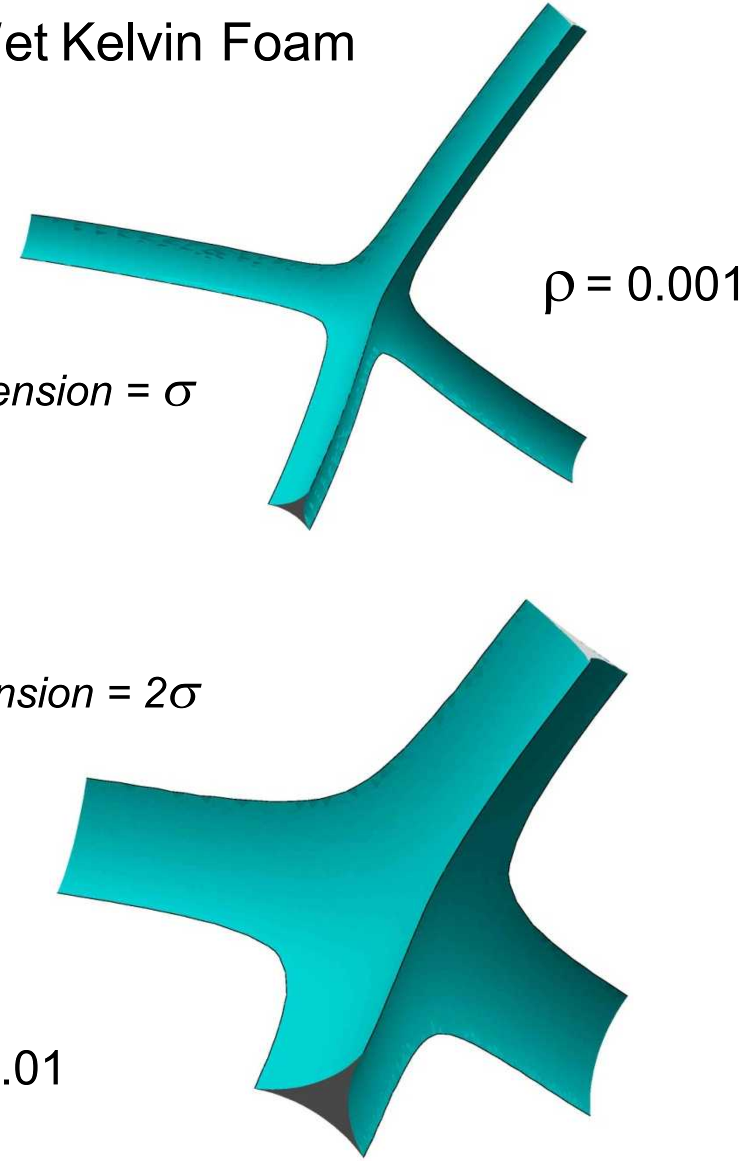

Plateau borders in liquid foams correspond to struts in solid foams

Modeling the strut-level geometry of open-cell foams

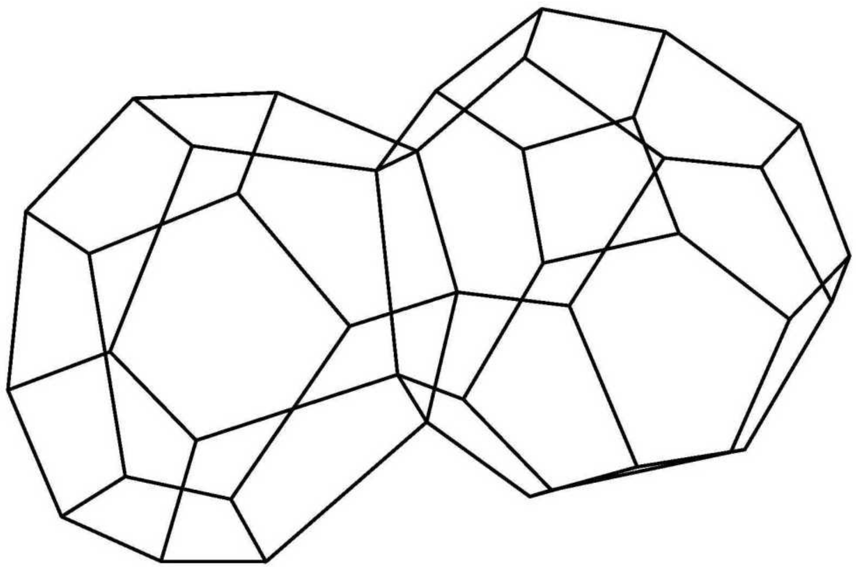

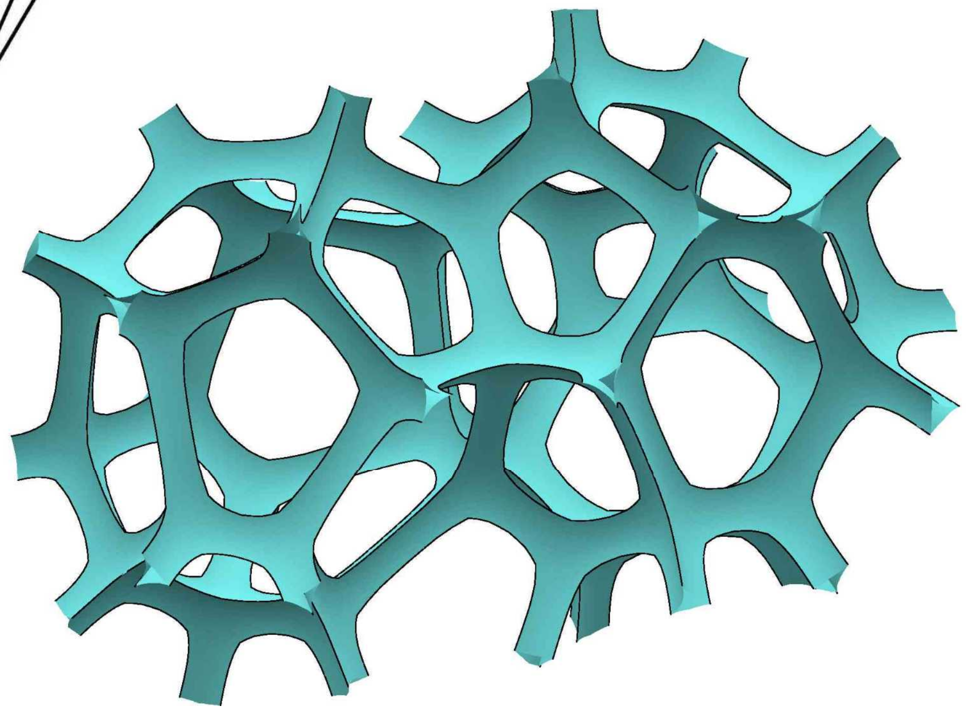

Random Monodisperse Foam

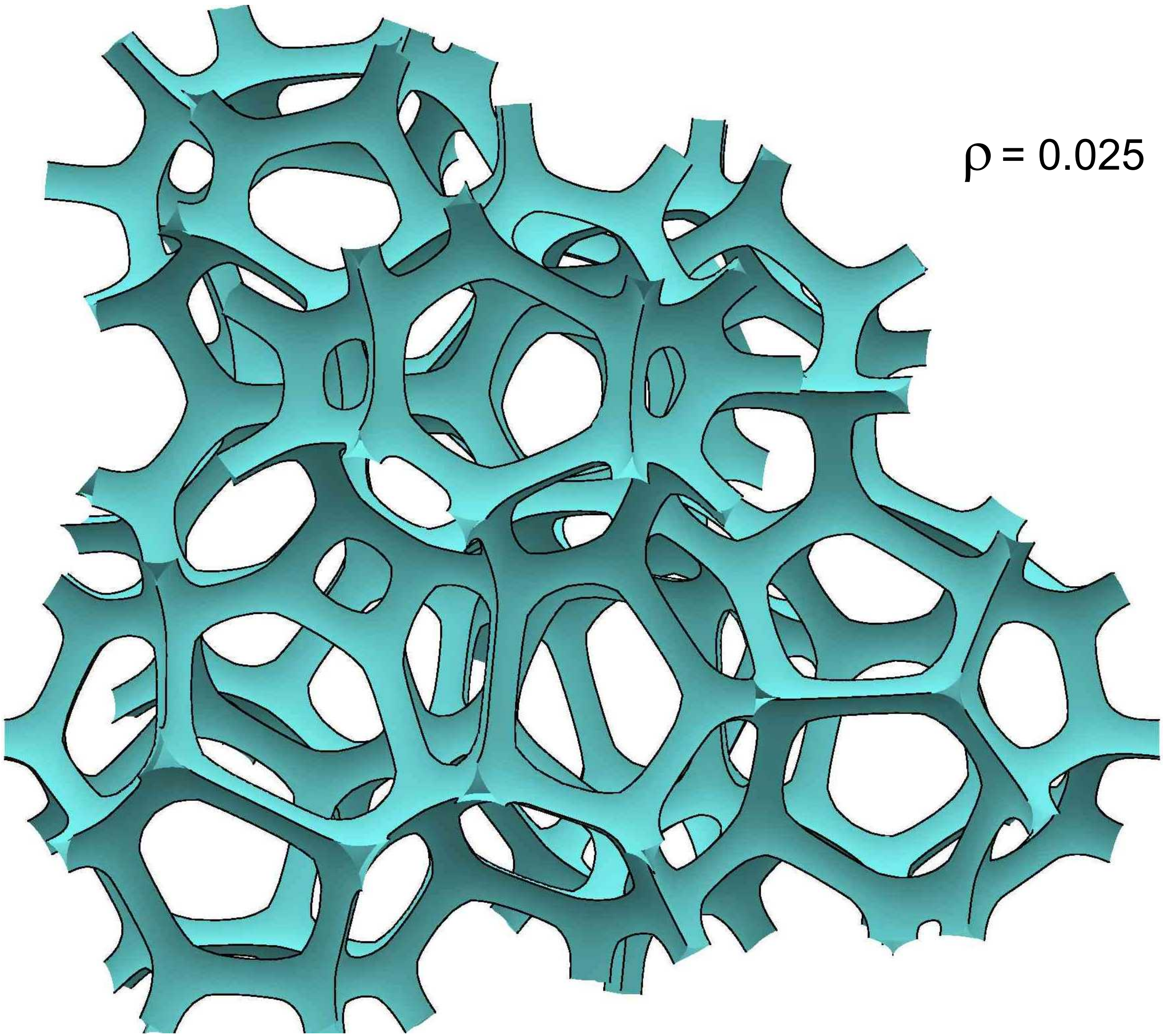

Evaluating the Cross-Section at Strut Midpoints

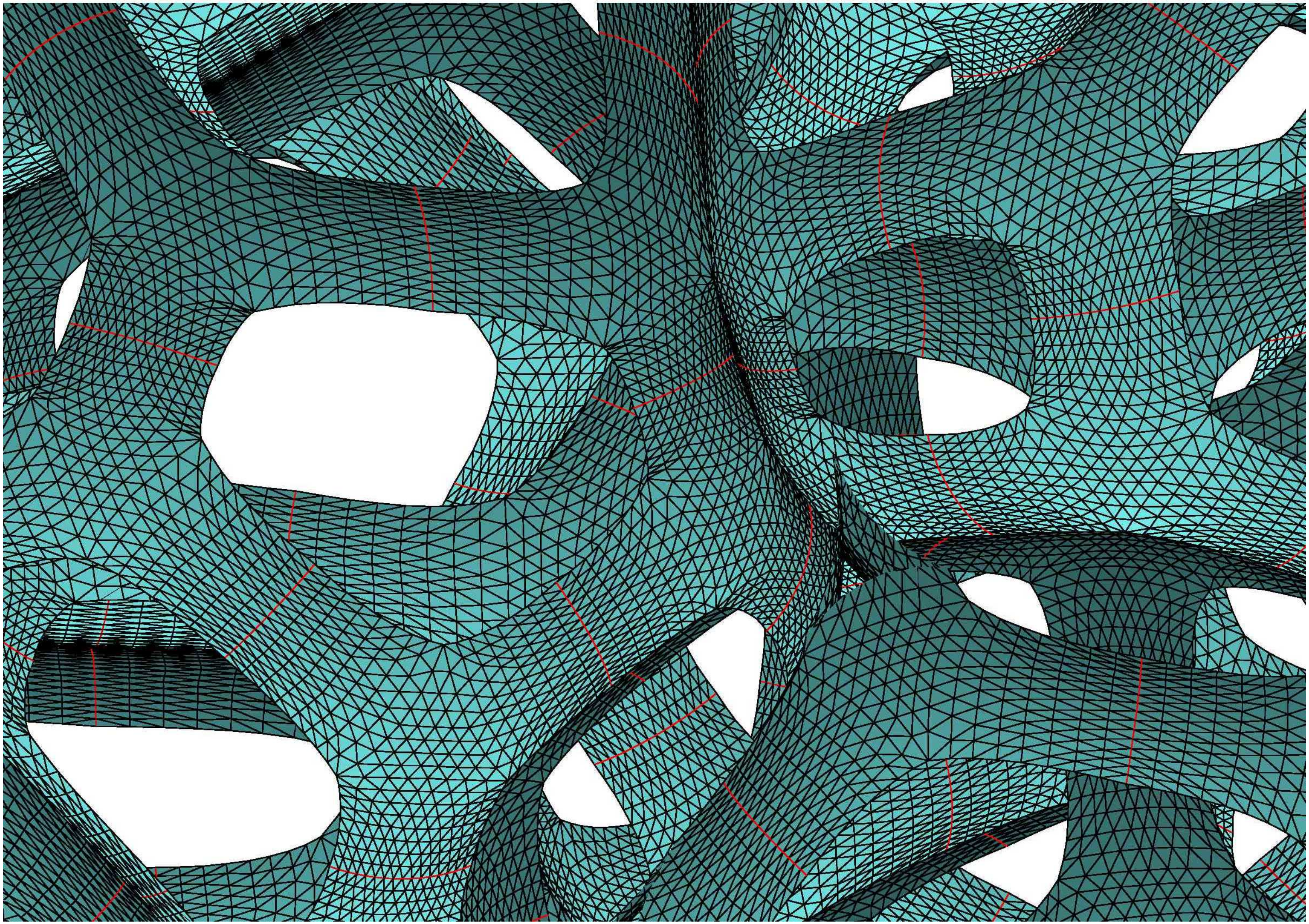

Evaluating the Cross-Section at Strut Midpoints

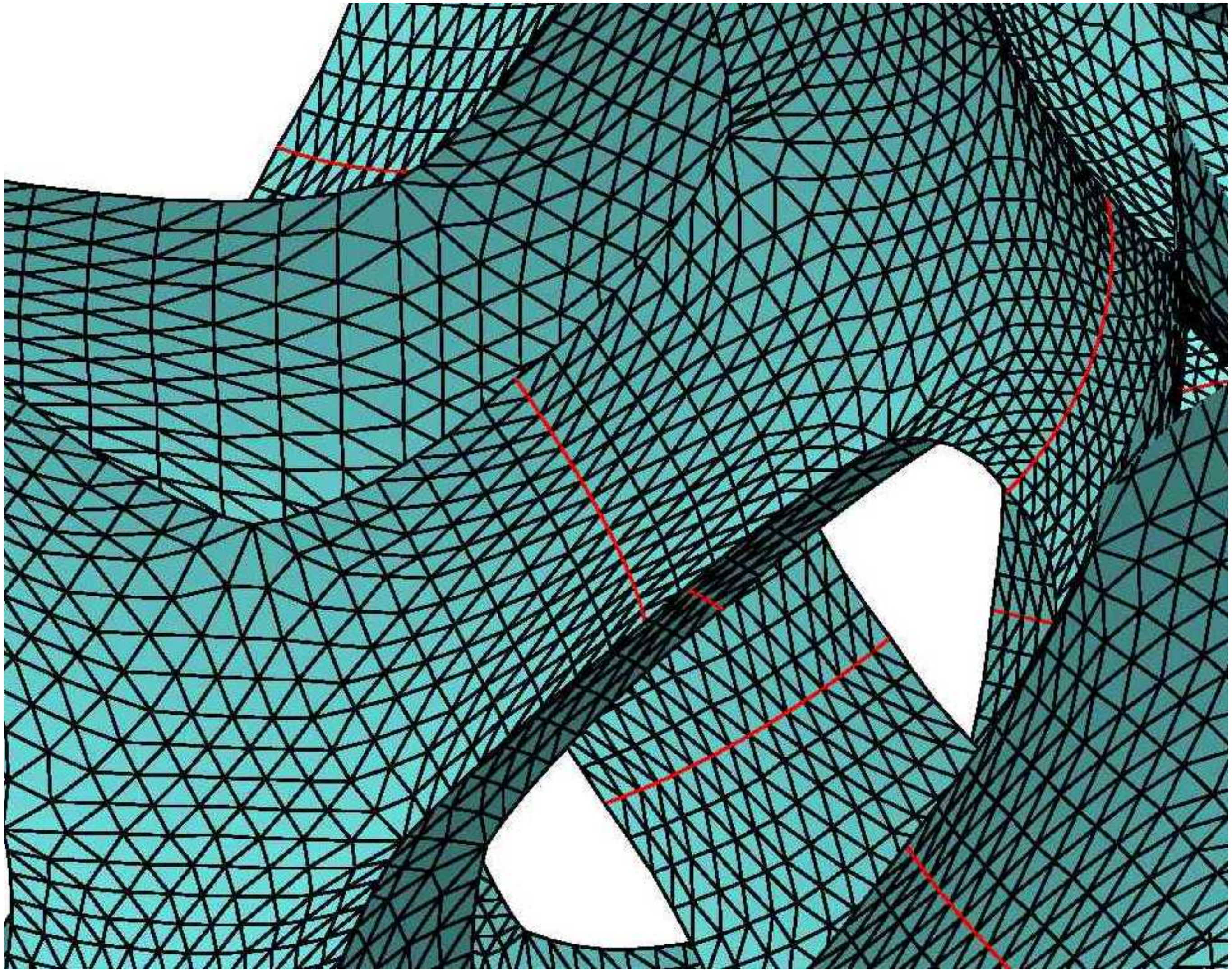

Cross-Sectional Area at Strut Midpoints

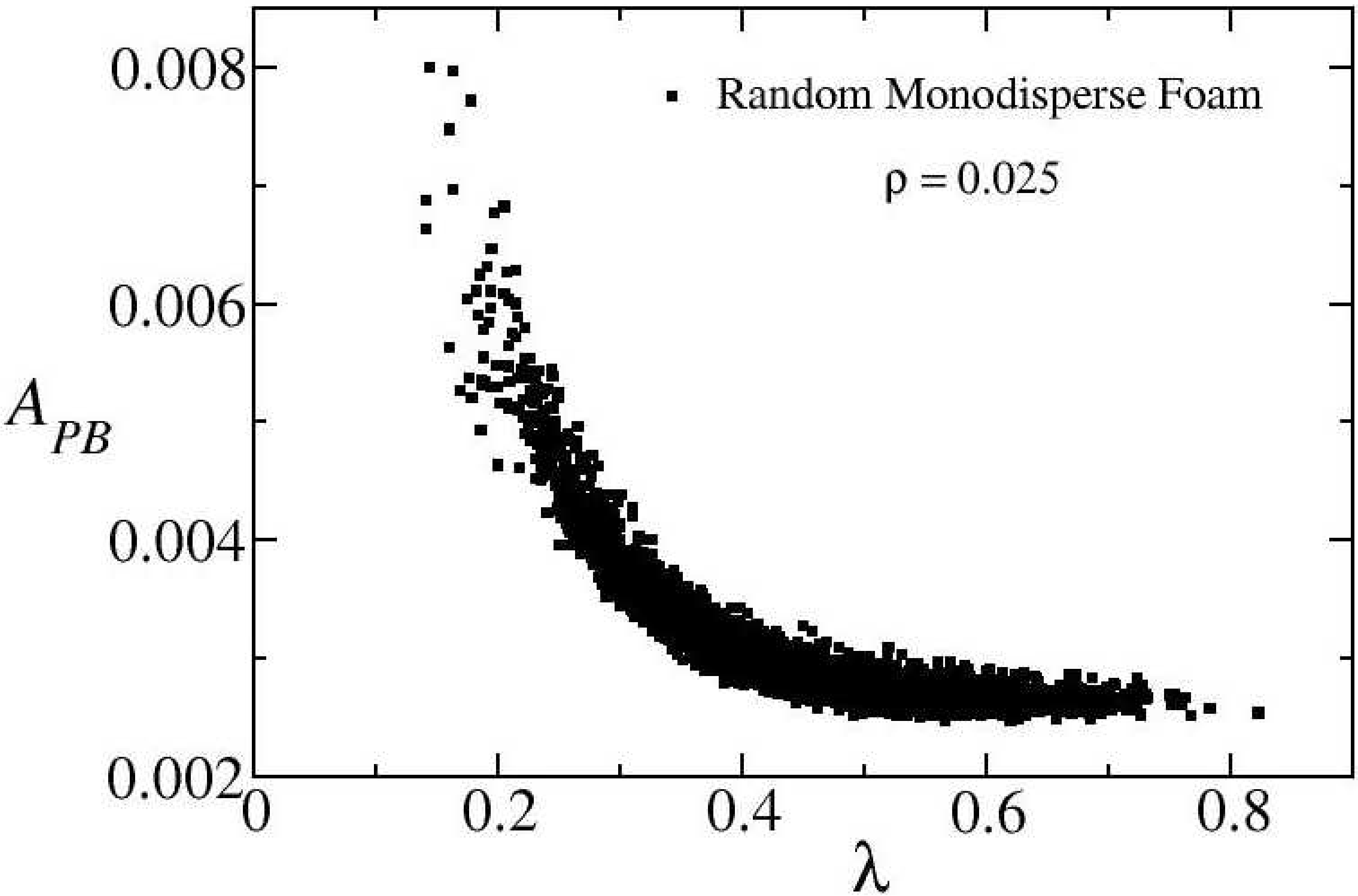

Material Distribution in Struts

Kyriakides and Jang, UT, Austin

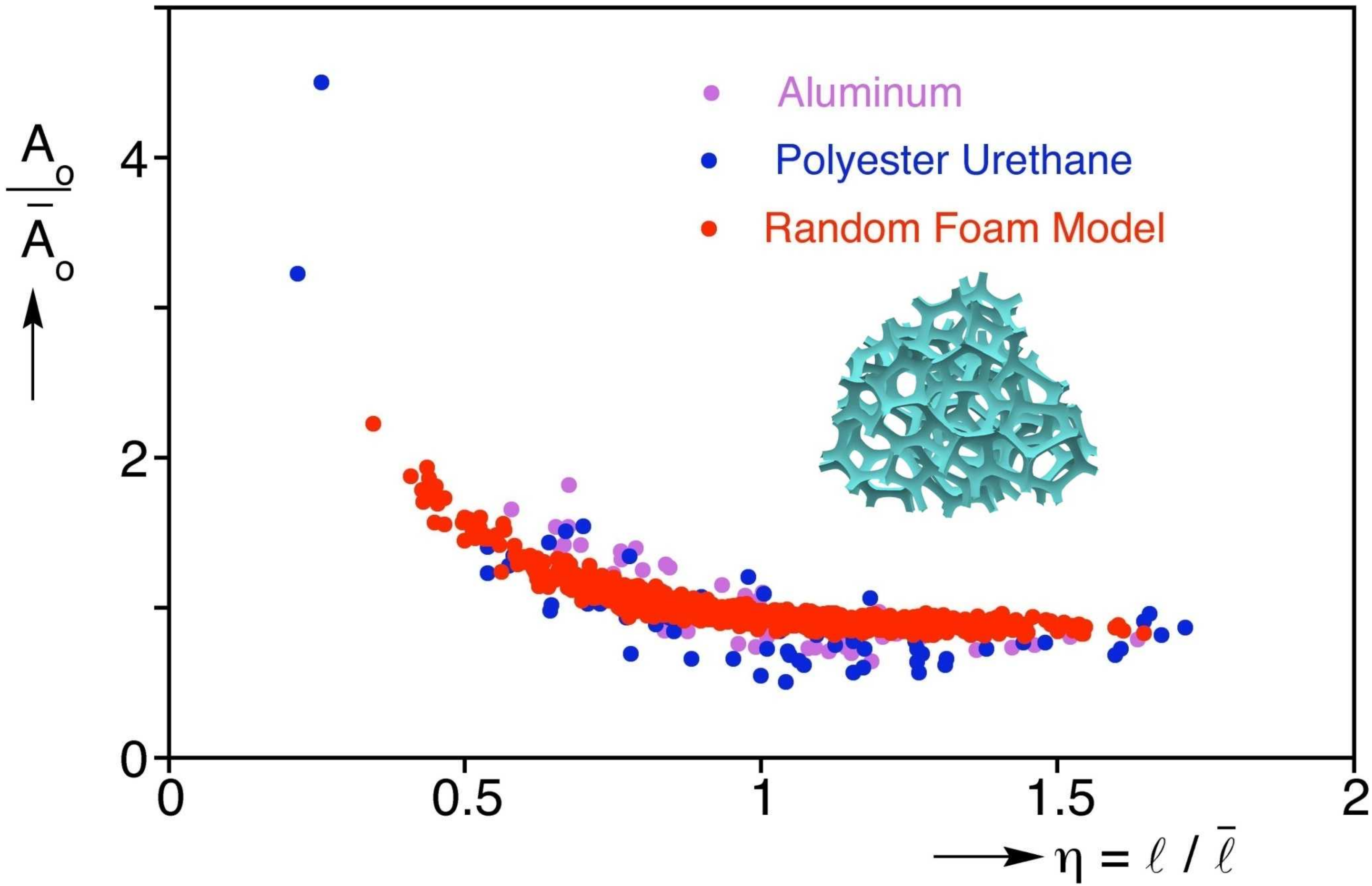

Realistic models of foam structure enable
prediction of structure-property-processing relationships
development of constitutive models

What are the important characteristics of foam structure?
How much do they influence foam properties?

Which models of foam structure are realistic?
Which are useful?

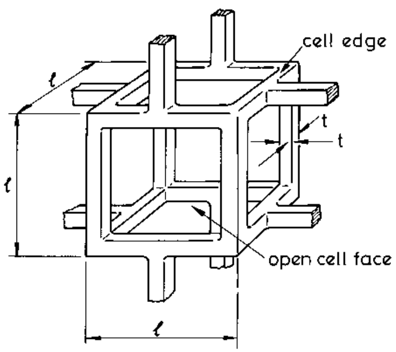

$$\frac{E^*}{E_s} \approx \left(\frac{\rho^*}{\rho_s}\right)^2$$

$$\frac{G^*}{E_s} \approx \frac{3}{8}\left(\frac{\rho^*}{\rho_s}\right)^2$$

$$\nu^* \approx \frac{1}{3}$$

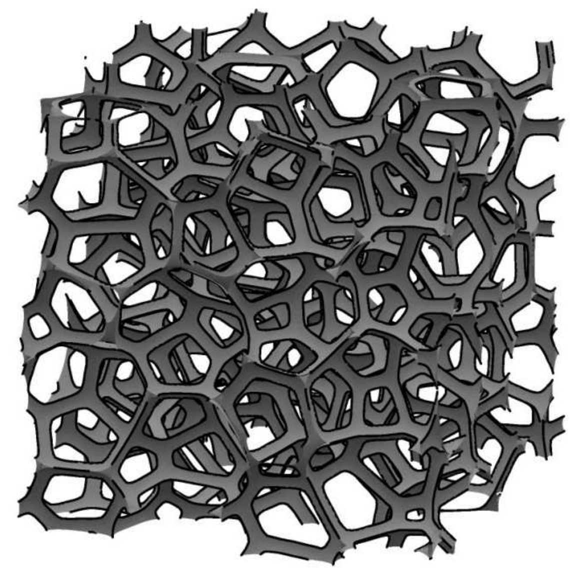

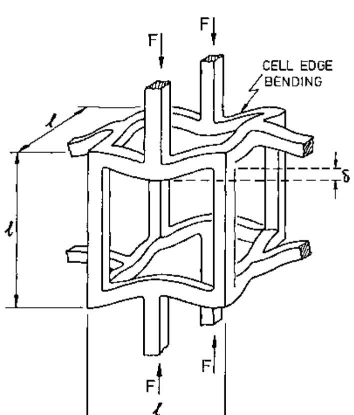

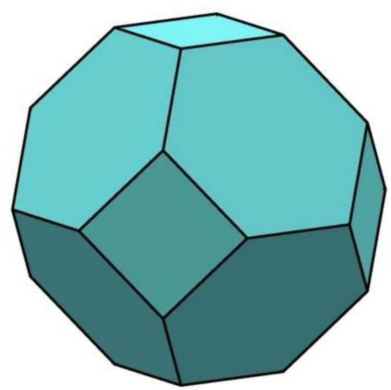

Animation by Dave Hensinger

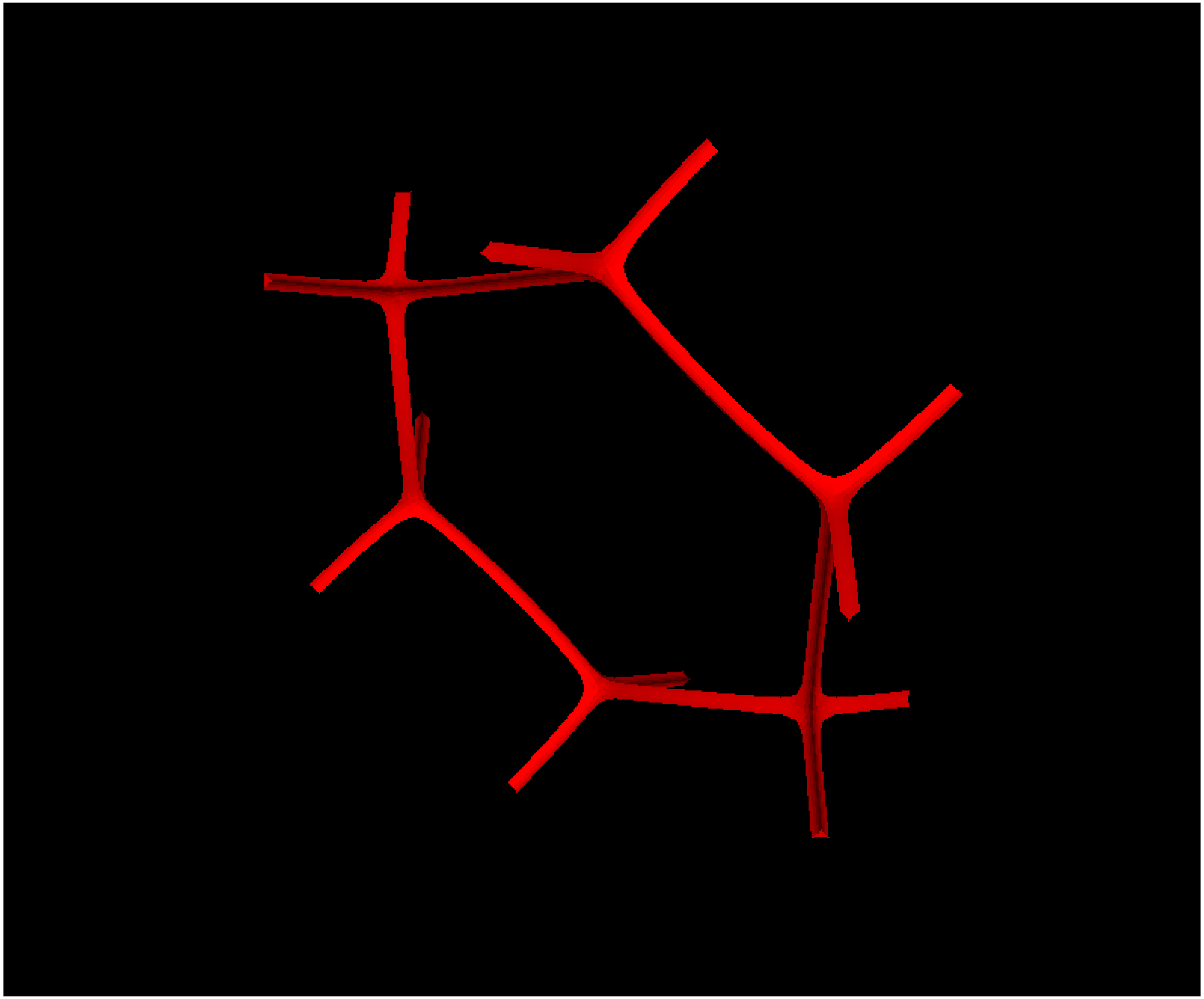

Microstructure of Open-Cell Kelvin Foam

Simple model based on triangular struts

Dave Hensinger

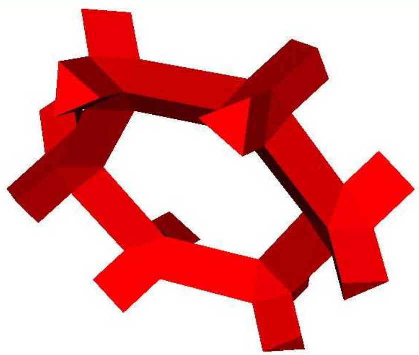

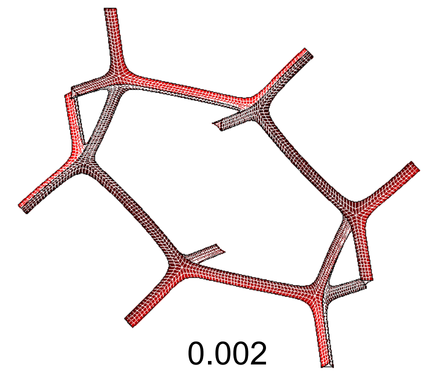

0.002

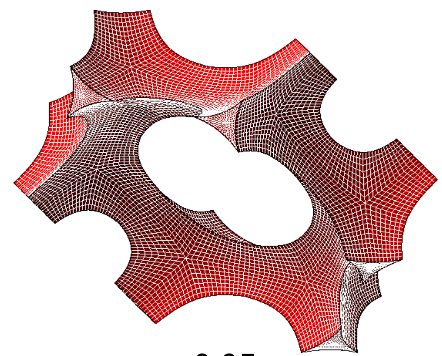

0.05

Use Surface Evolver to calculate the shape of Plateau borders in liquid foam.

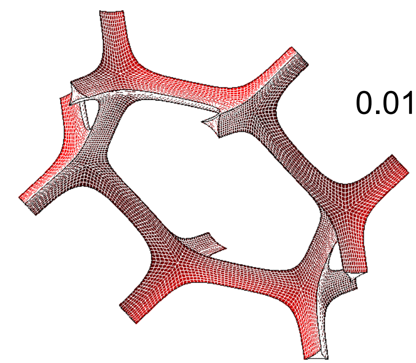

0.01

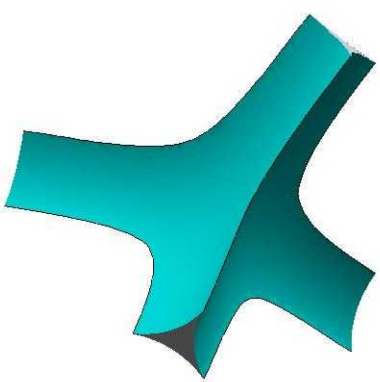

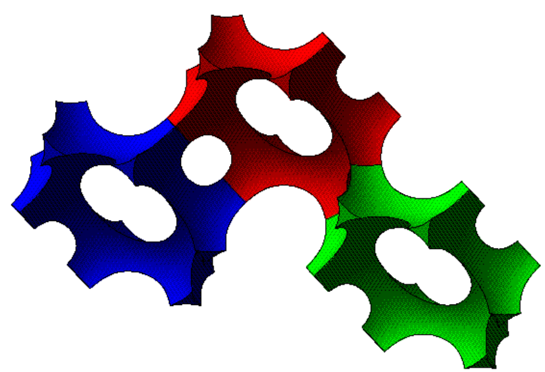

Polyester Urethane (PU) Foams

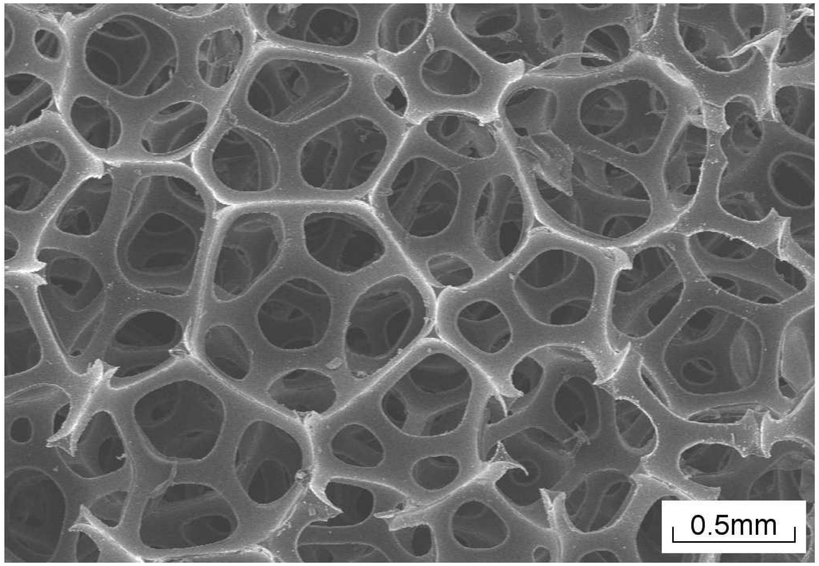

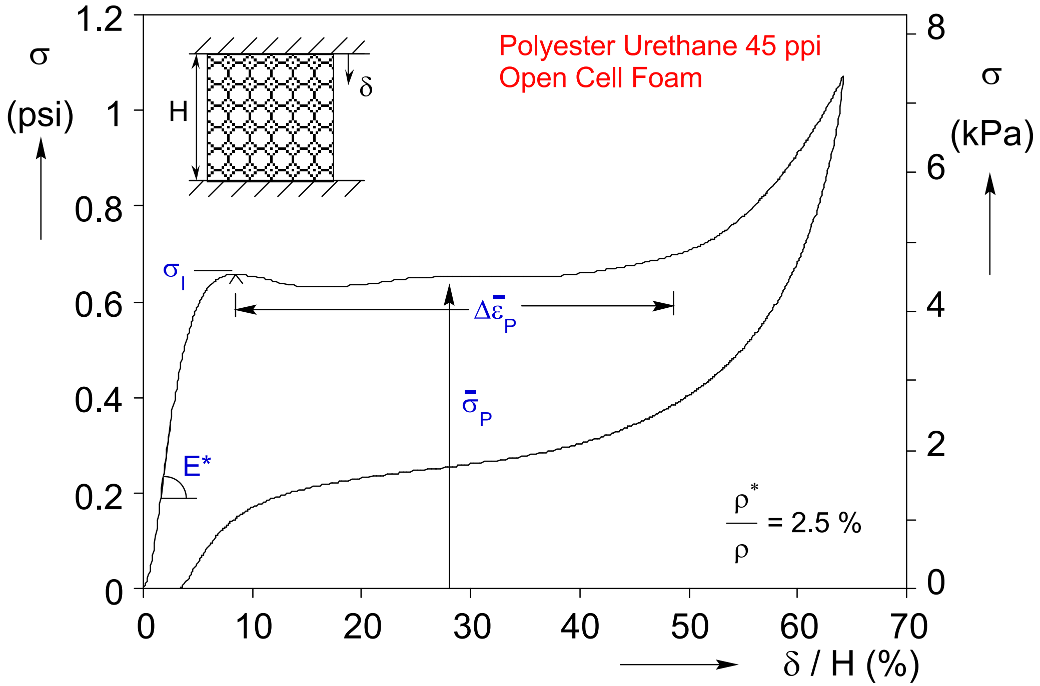

100 ppi, $\frac{\rho^*}{\rho} = 2.82\ (\%)$

Compressive Response

Polyester Urethane Foam Morphology

Micro-Computed X-ray Tomography: Scanco μCT 80

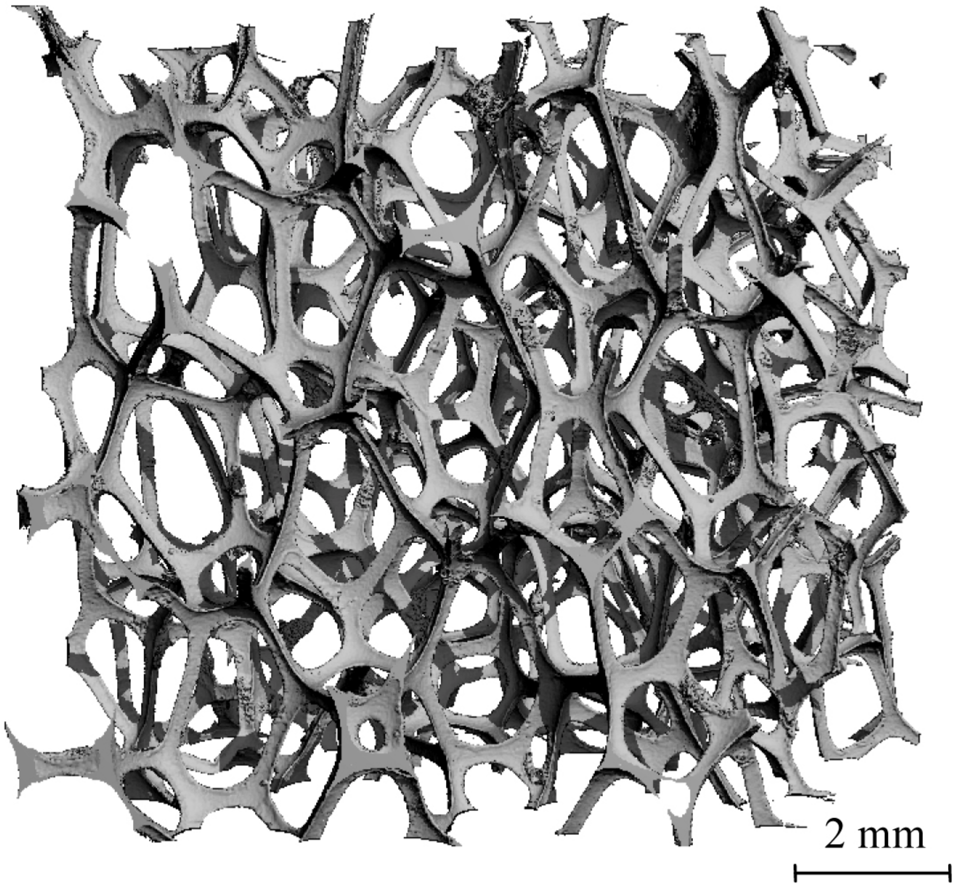

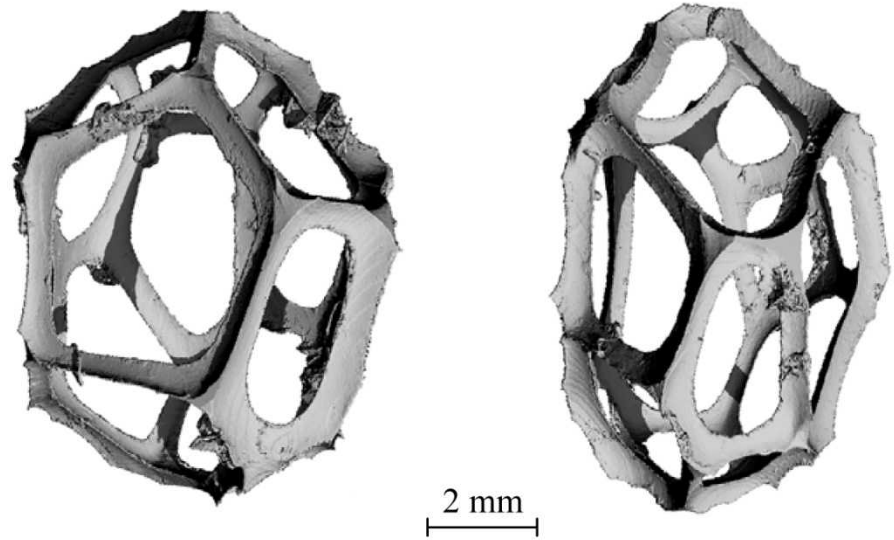

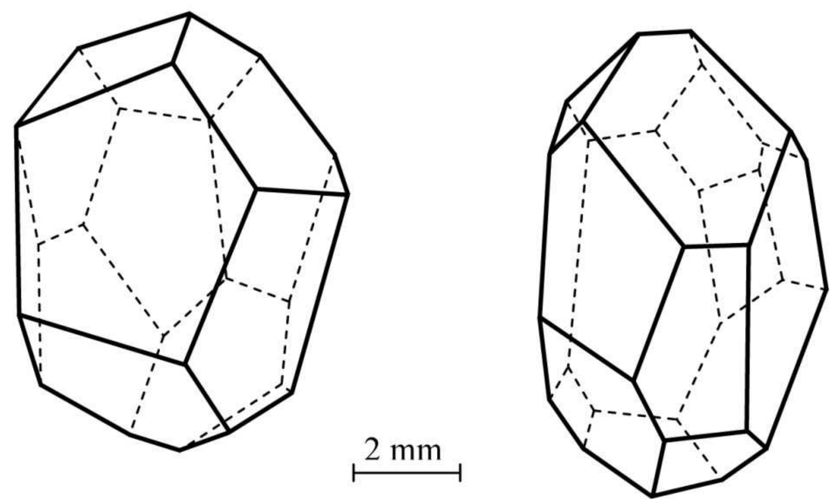

3-ppi $\frac{\rho^*}{\rho} = 2.2\ \%$

PU Microstructure

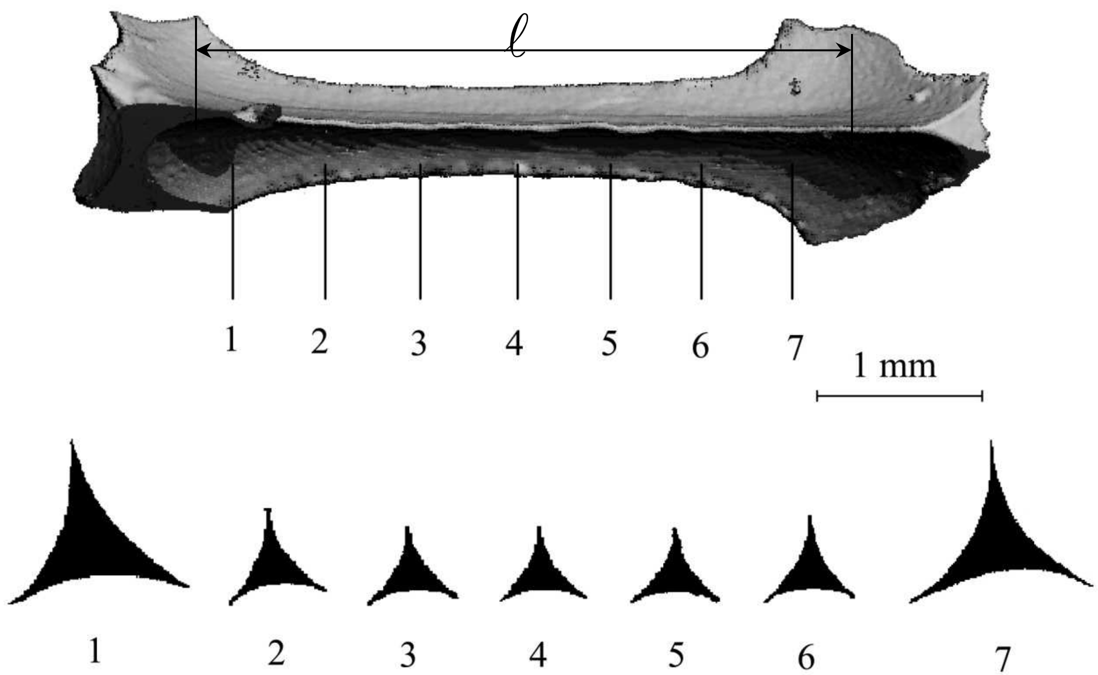

Ligament

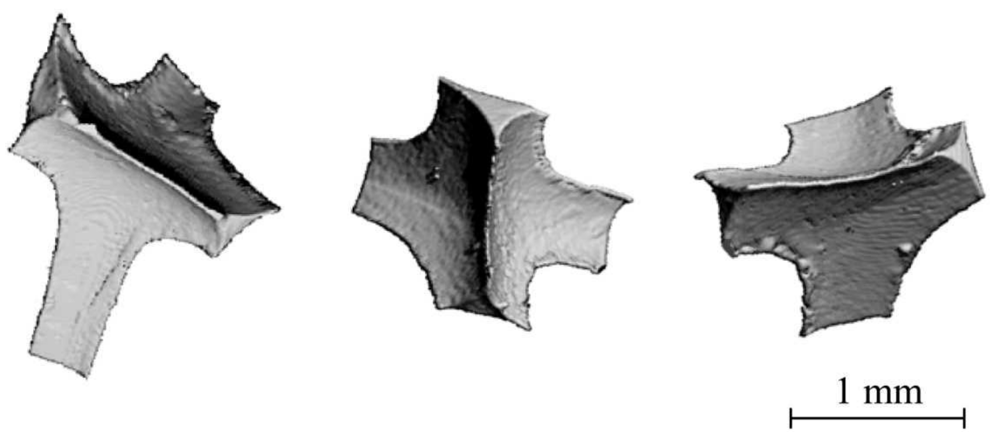

Nodes

PU Ligament Geometry

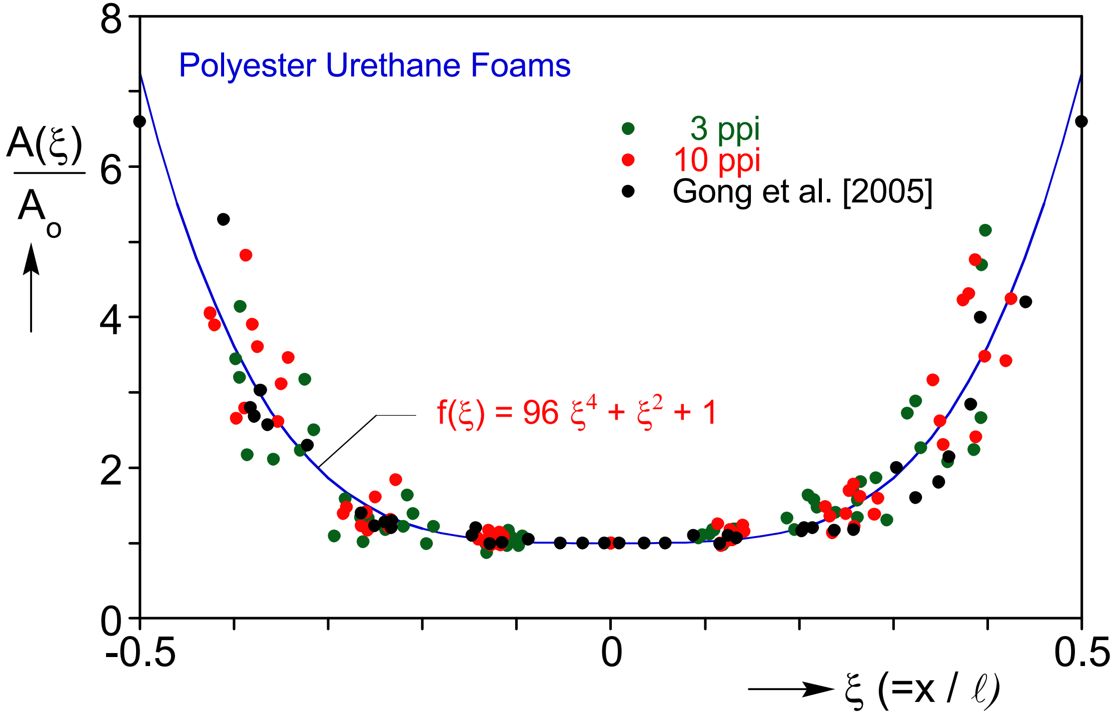

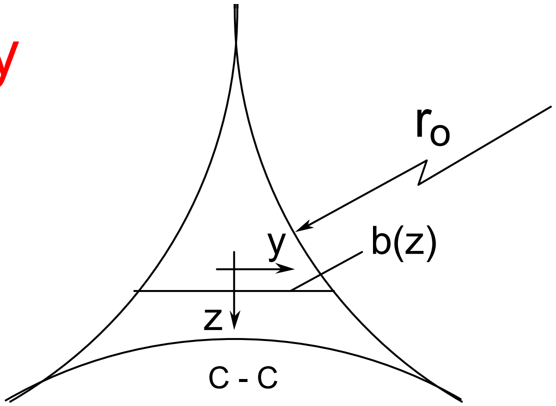

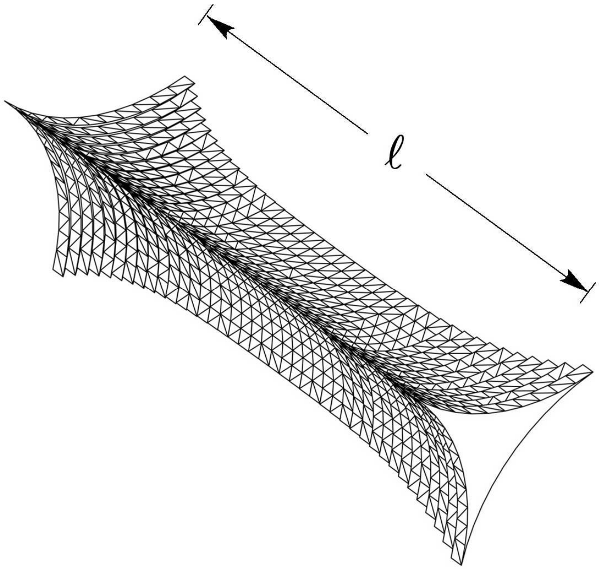

$$A(\xi) = A_o f(\xi) = A_o \left[96\xi^4 + \xi^2 + 1 \right]$$

Crushing of PU Foam

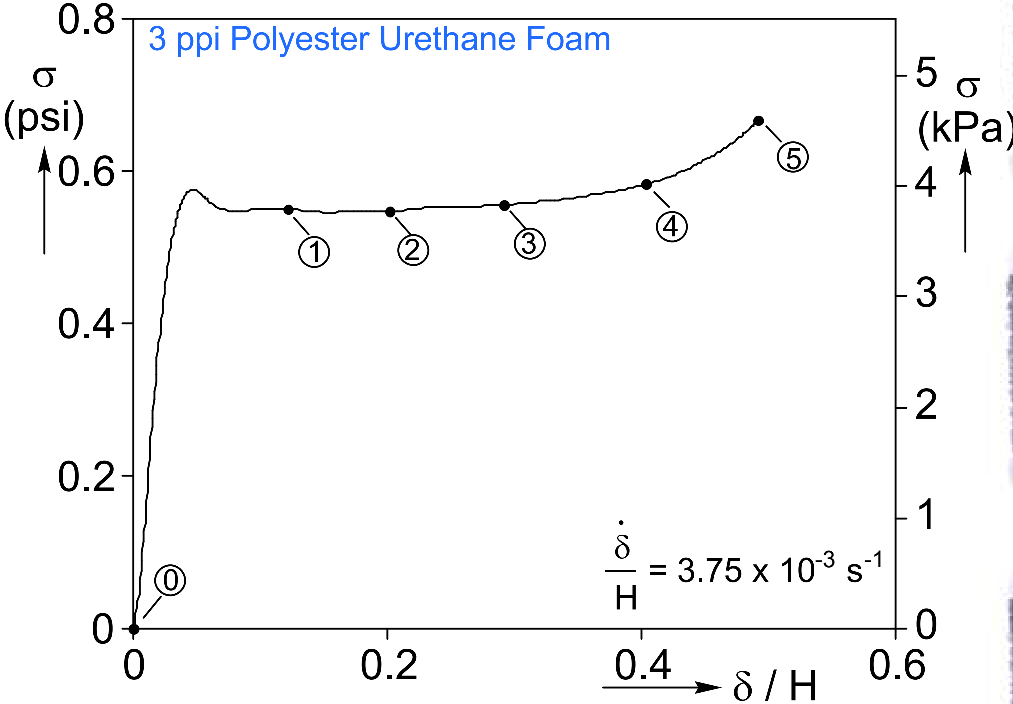

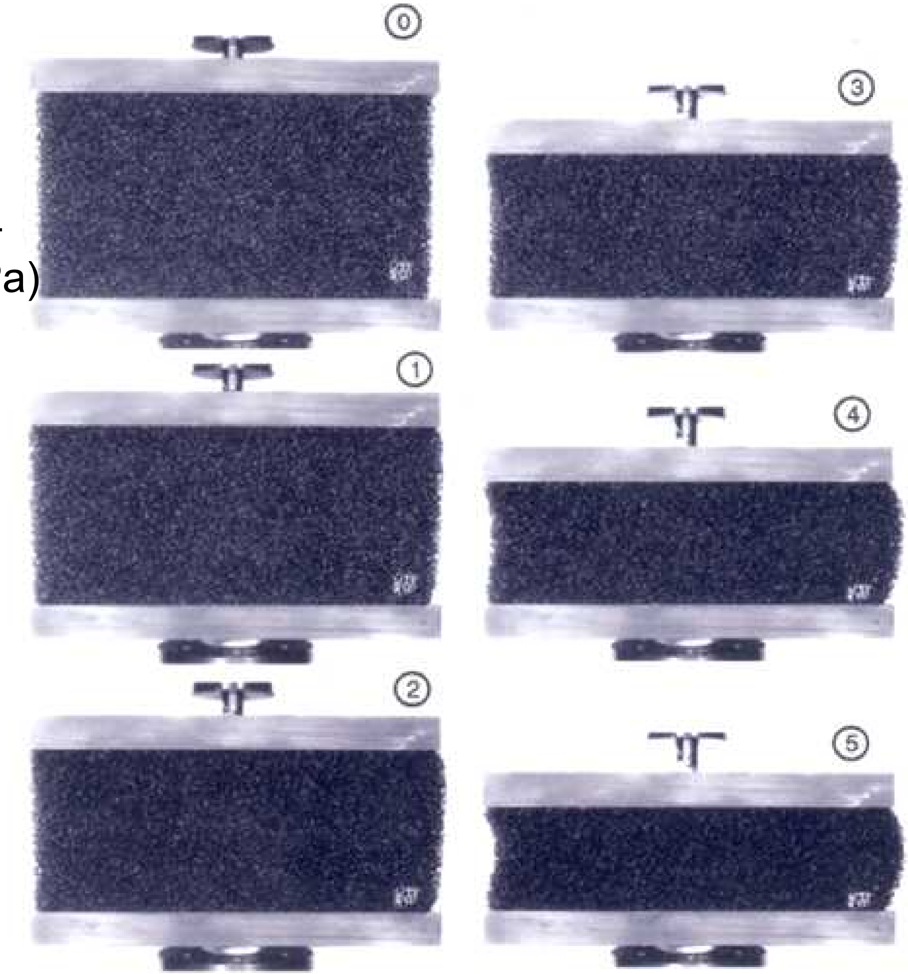

PU Anisotropy

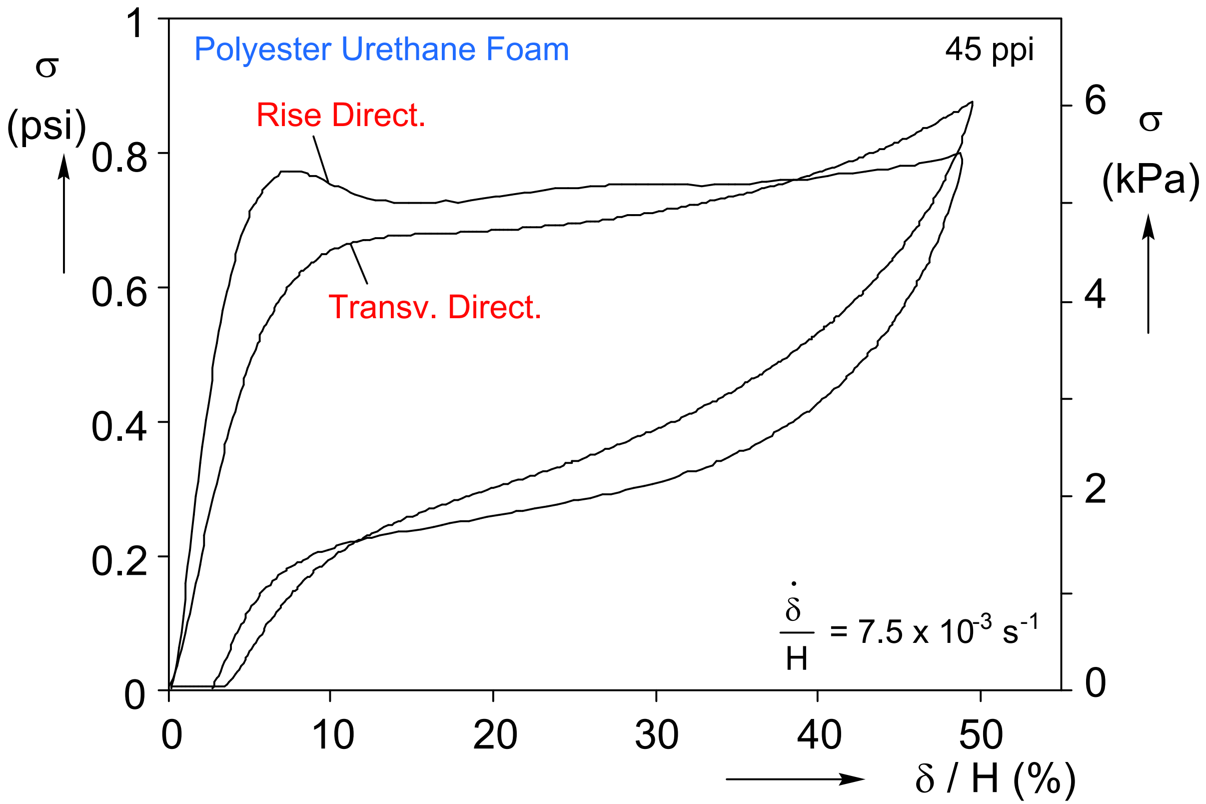

Anisotropic Kelvin Cell

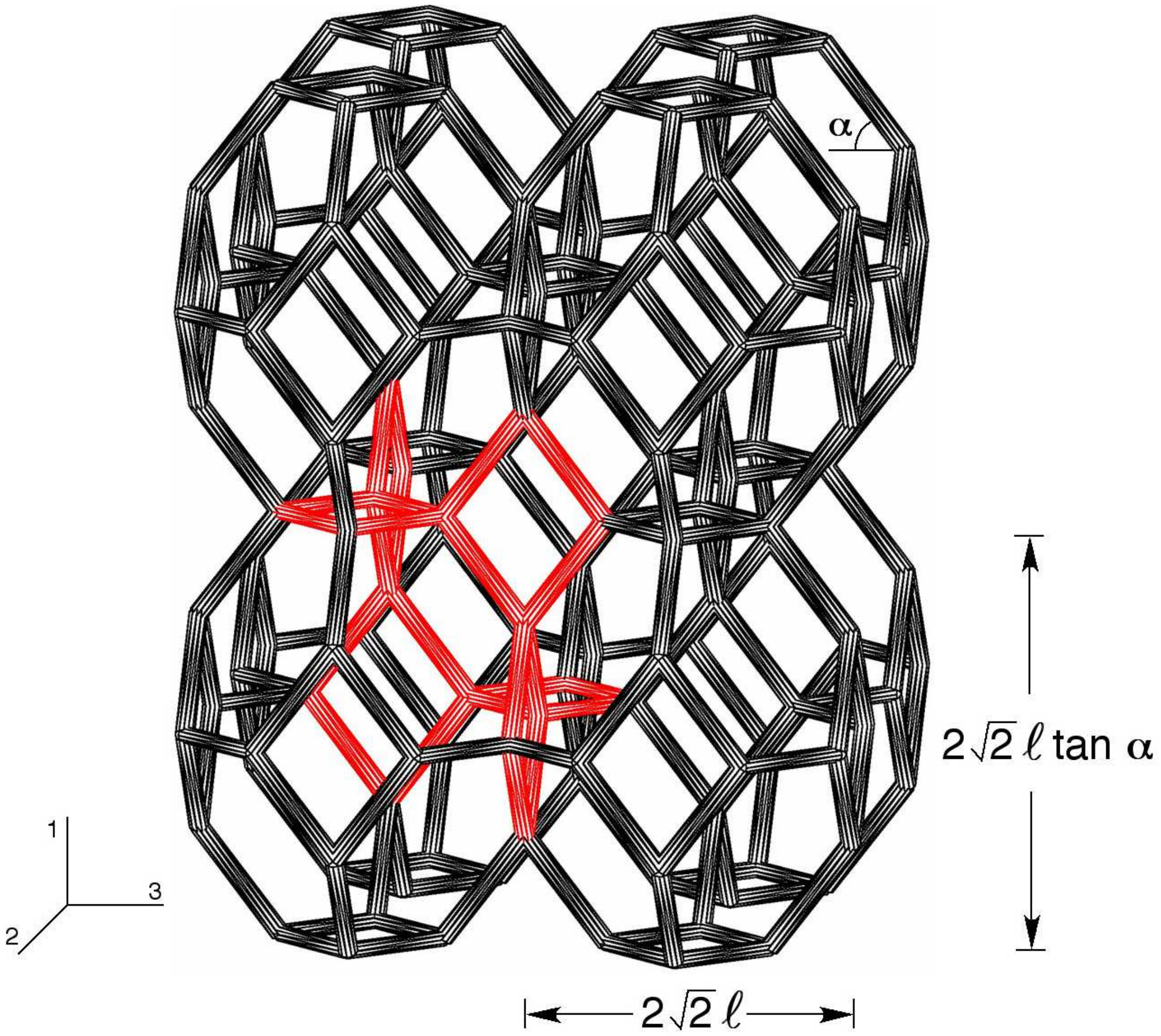

$$\lambda = \frac{h_1}{h_2} = \tan\alpha$$

$$\alpha \geq \frac{\pi}{4}$$

Rise Direction Characteristic Domain Response (PU)

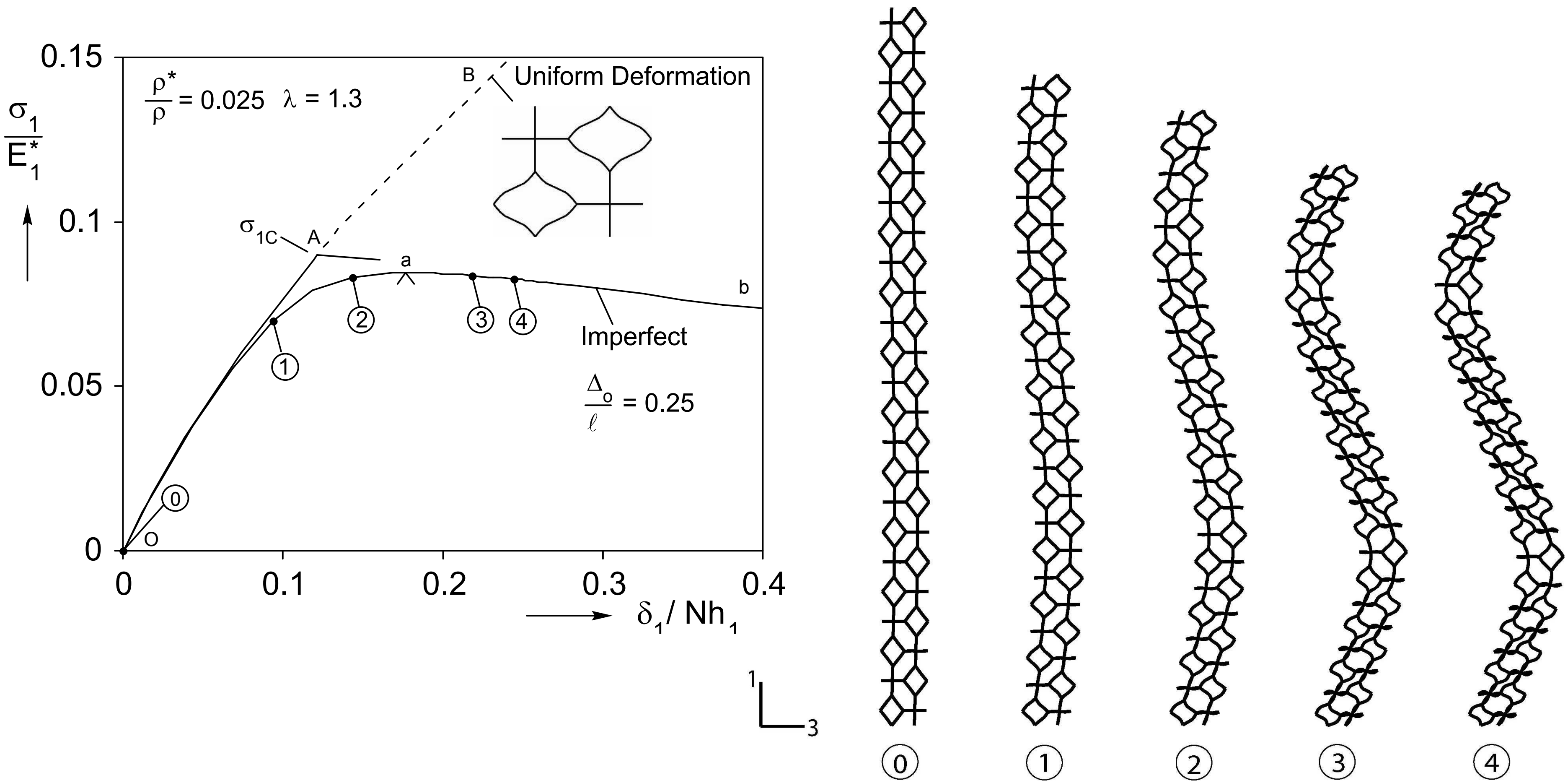

Gong et al., 2005

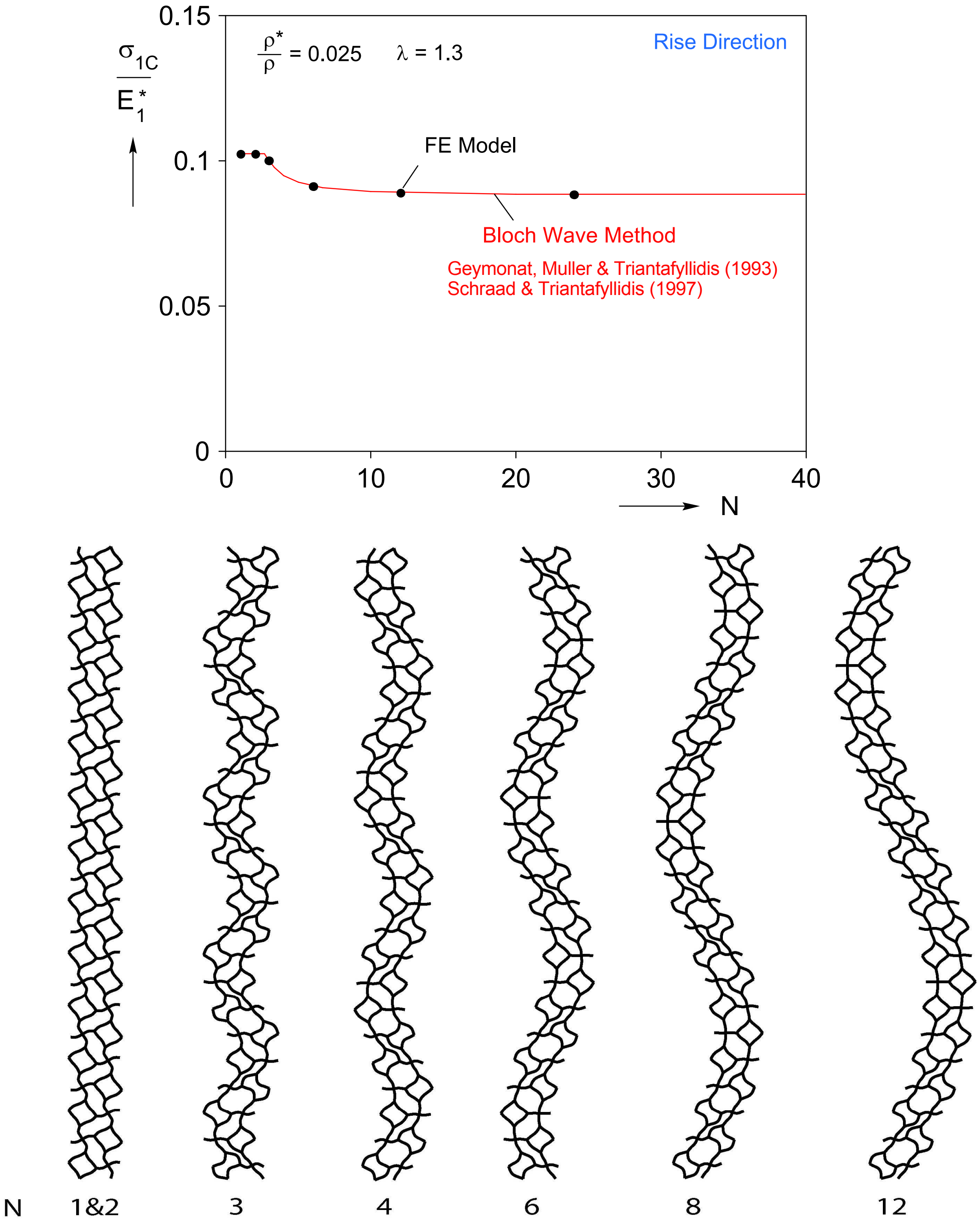

Transverse Direction Characteristic Cell Response

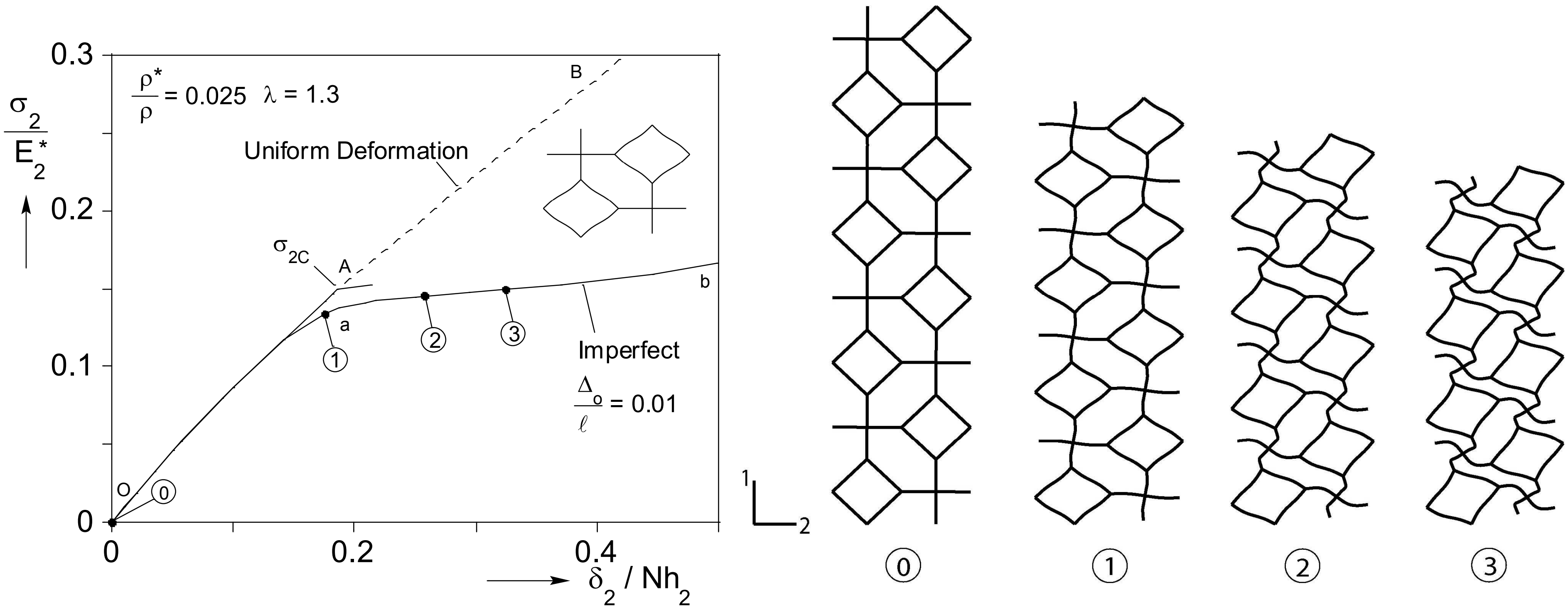

Crushing of Finite Size (12x28 Cells) PU Foam Model

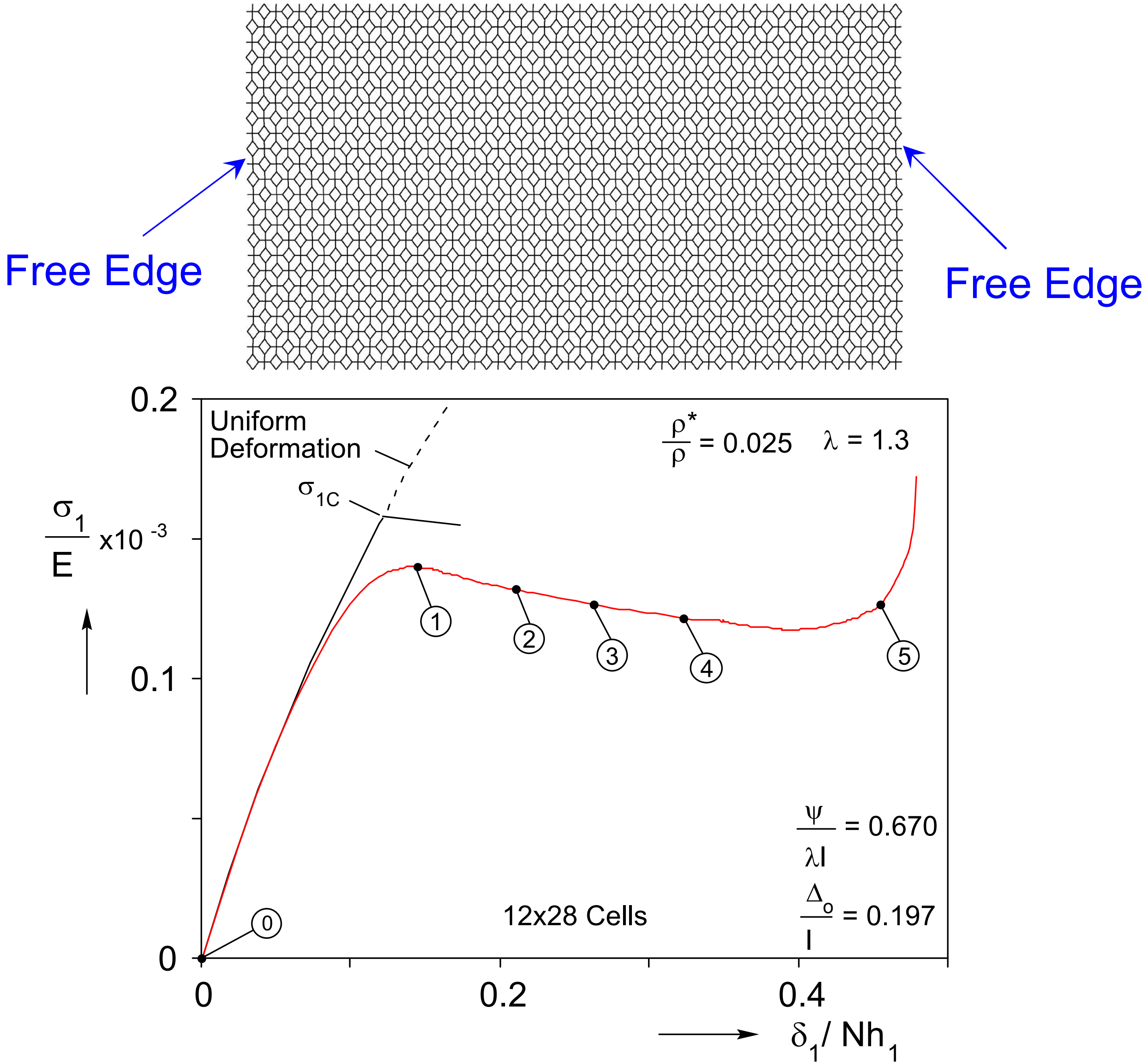

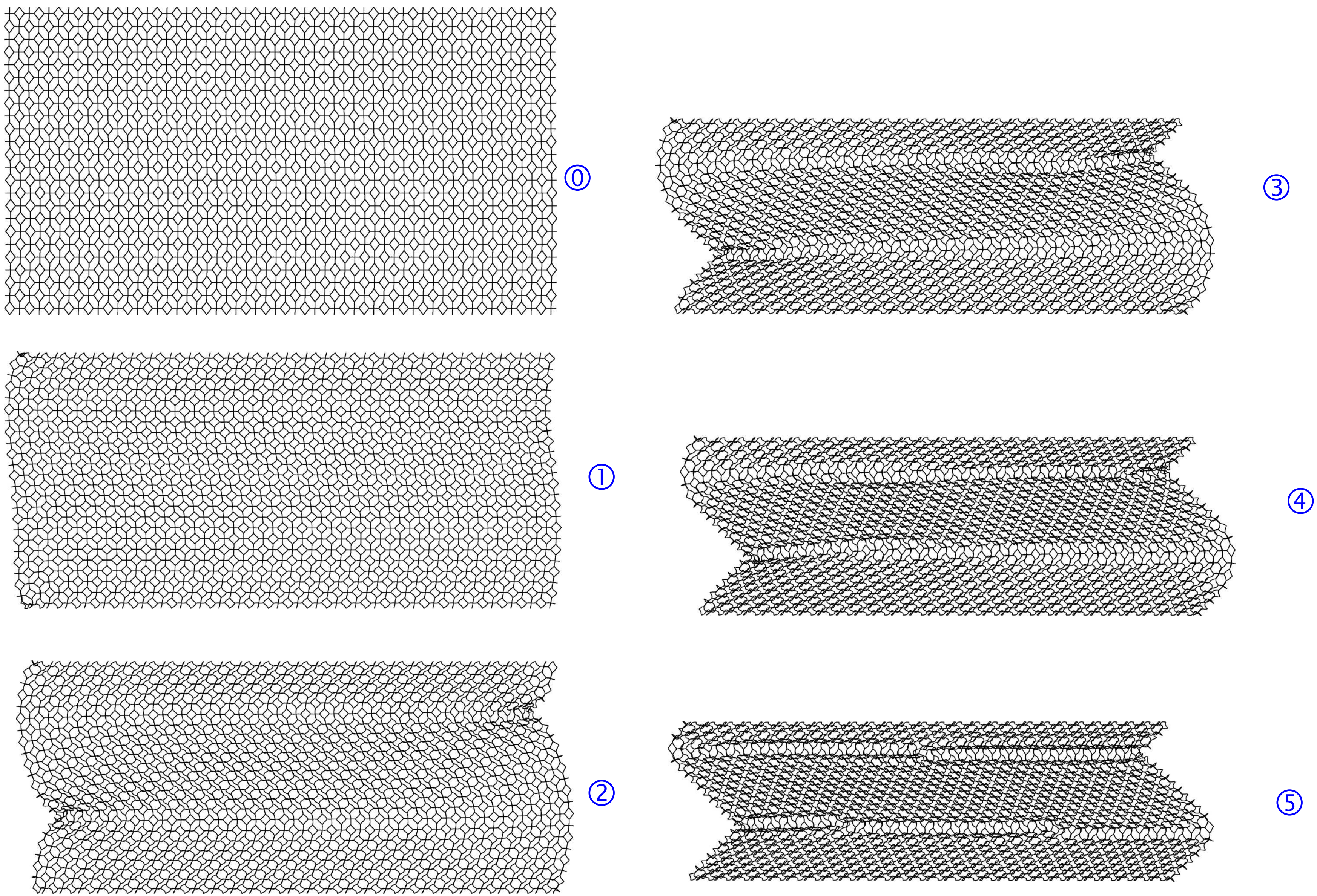
⓪
①
②
③
④
⑤

Aluminum Foam

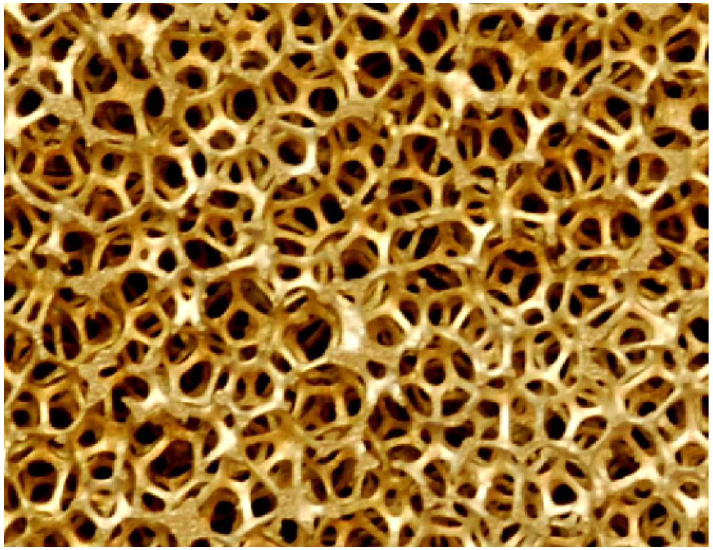

Al 6101-T6

40-ppi

$$\frac{\rho^*}{\rho} = 8.2\ \%$$

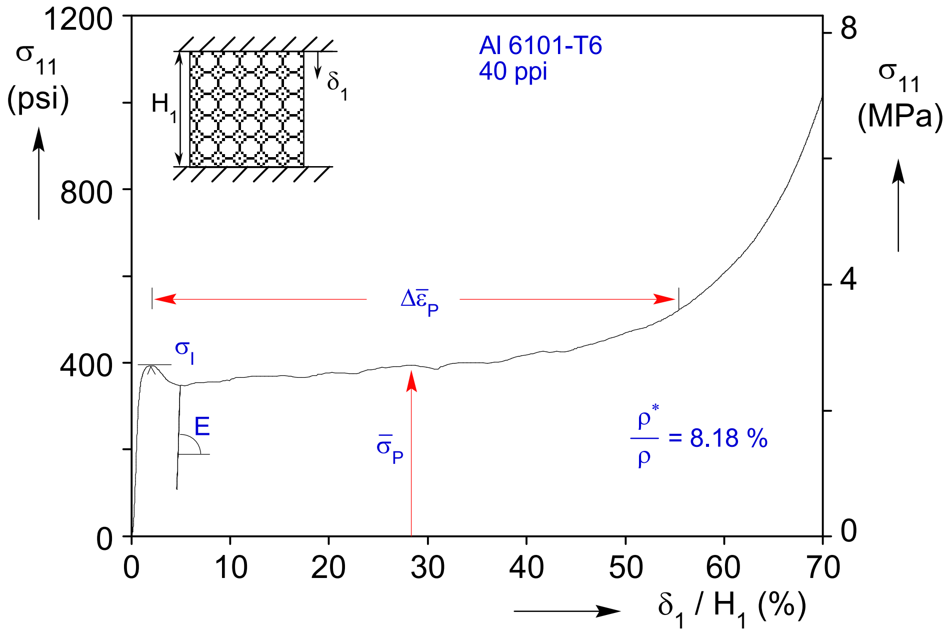

Compressive Response
Rise Direction

Al Microstructure

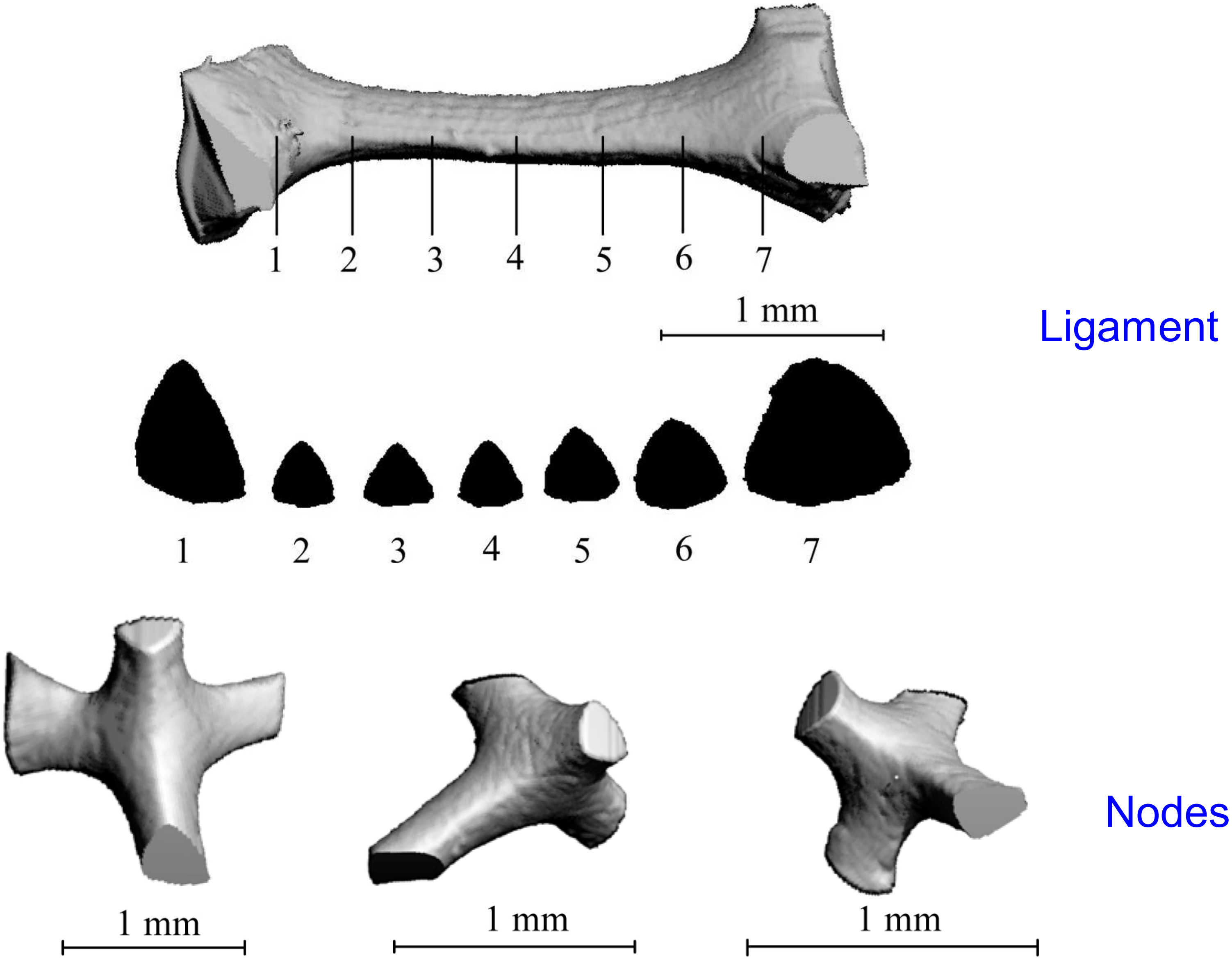

Al Ligament Geometry

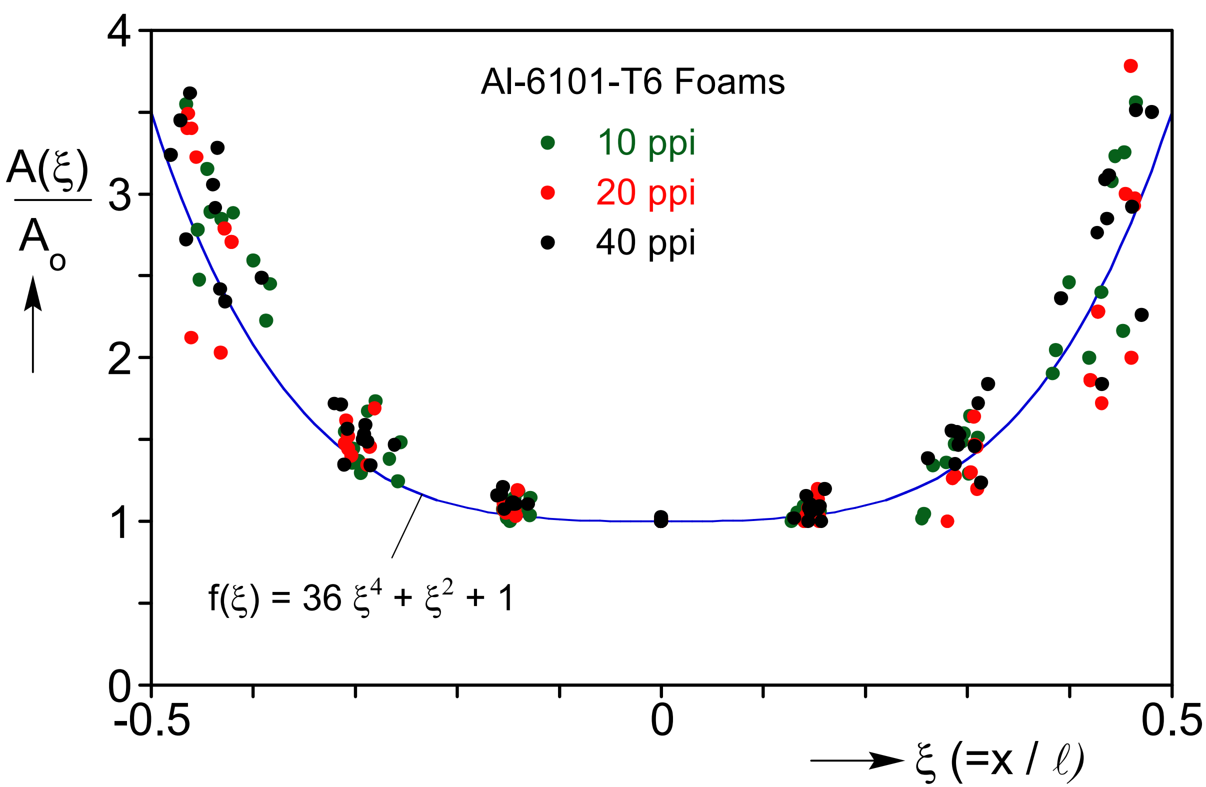

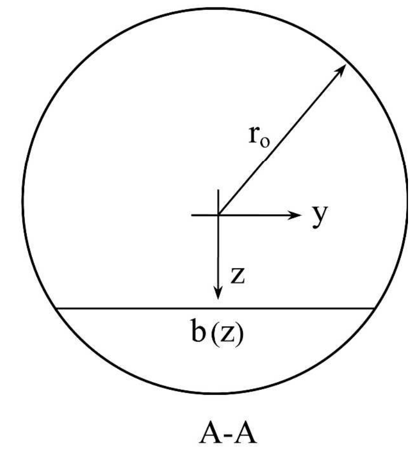

QuickTime™ and a TIFF (Uncompressed) decompressor are needed to see this picture.

$$A(\xi) = A_o f(\xi) = A_o \left[36\xi^4 + \xi^2 + 1 \right]$$

Crushing of 6x9x6 Cells Domain Al Foam

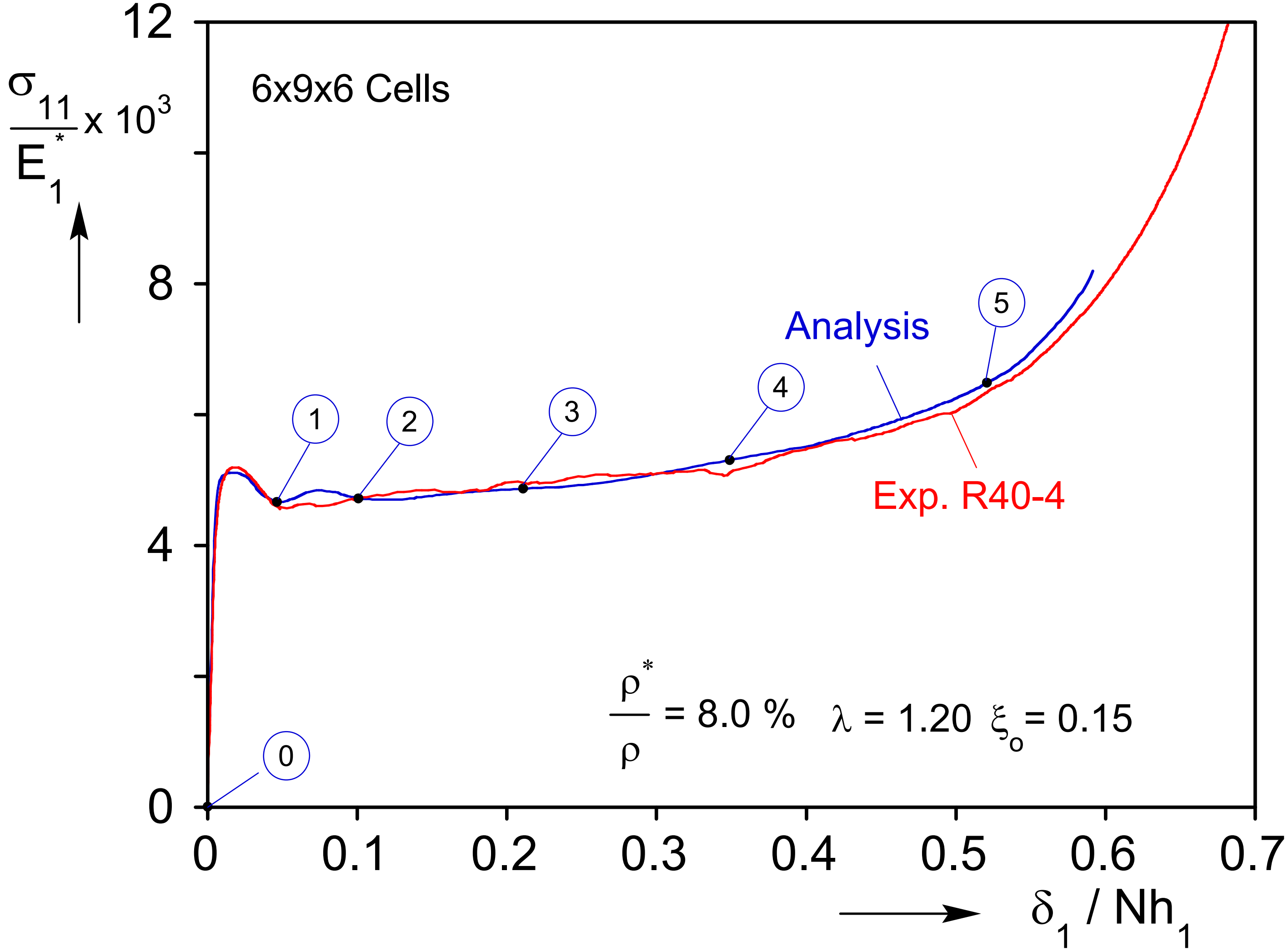

Internal X-Ray Tomography Images of Evolution of Crushing

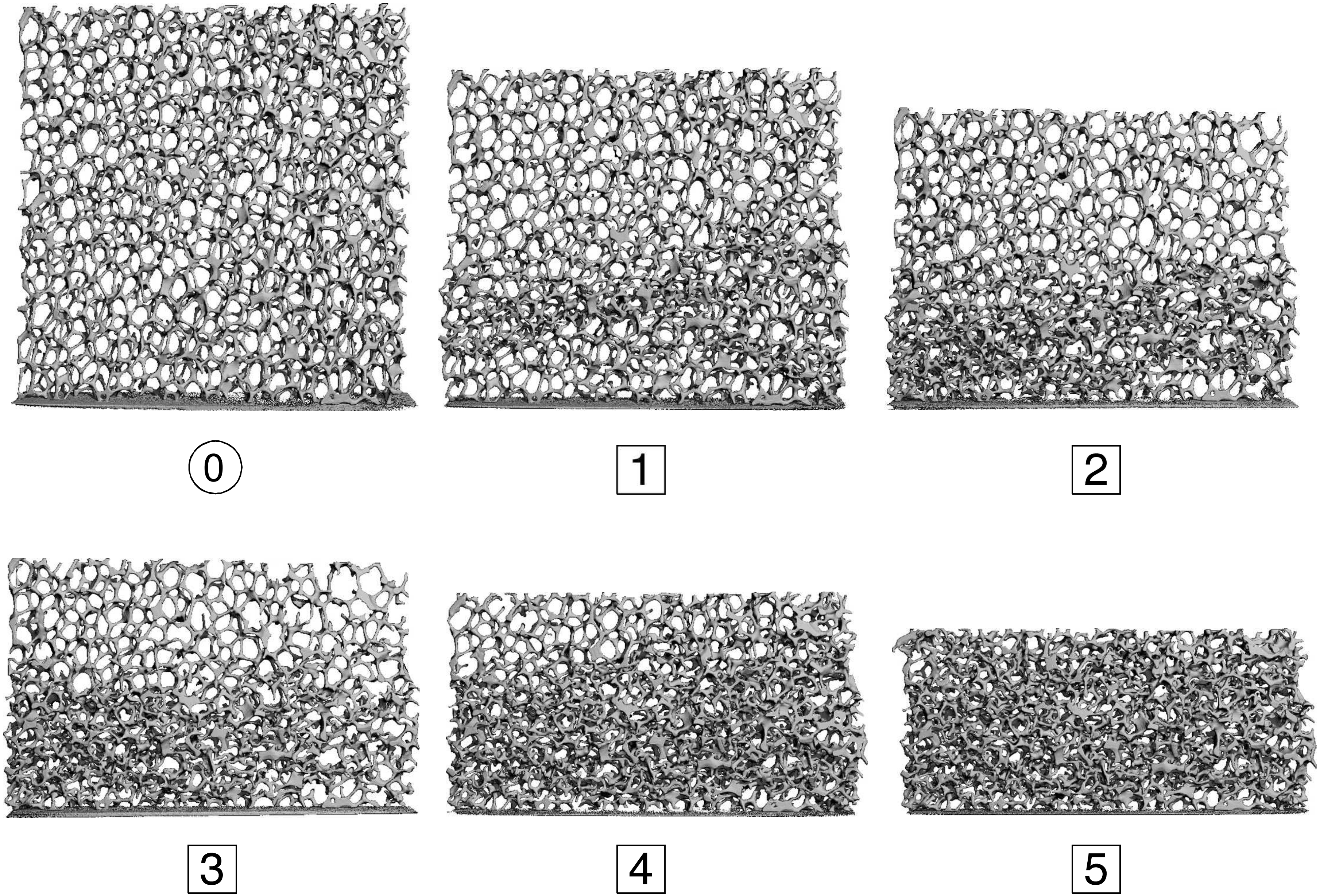

Al-6101-T6 Foam (ERG Duocel): 10-ppi $\frac{\rho^*}{\rho} = 8.2\ \%$

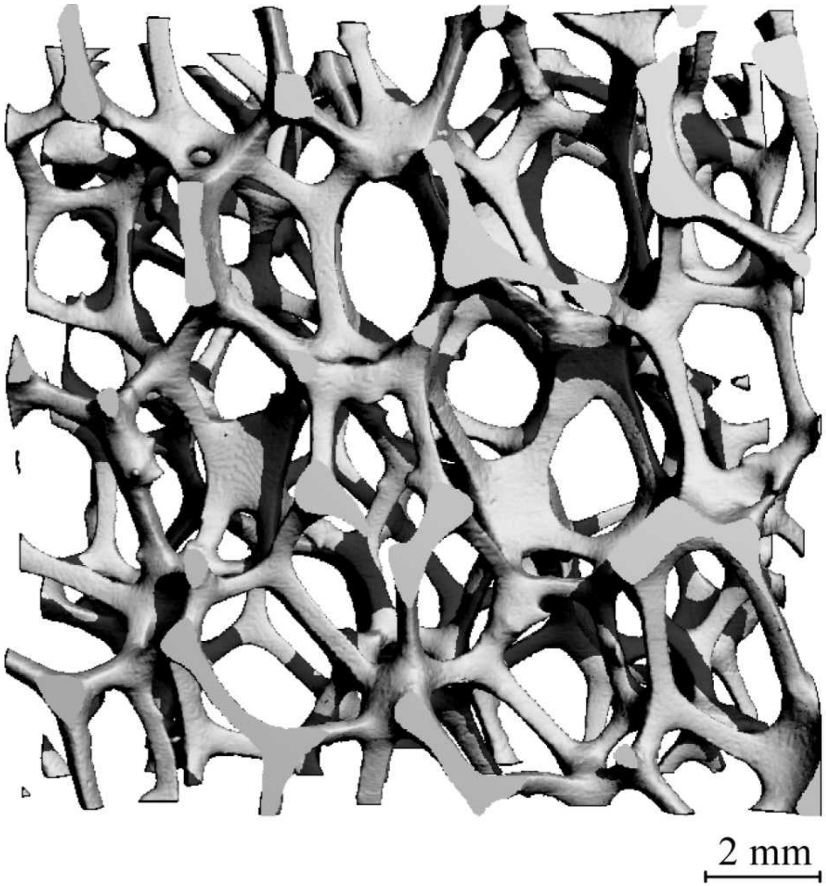

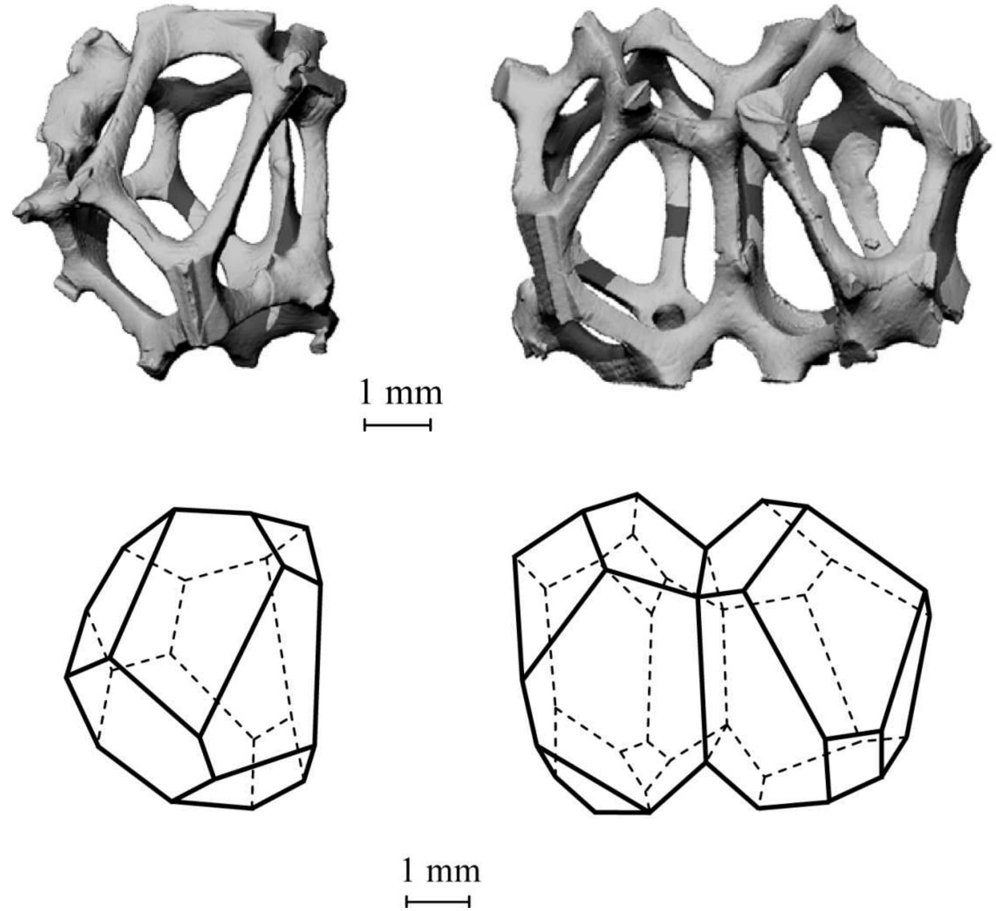

Crushing of Al Foam (Rise Direction)

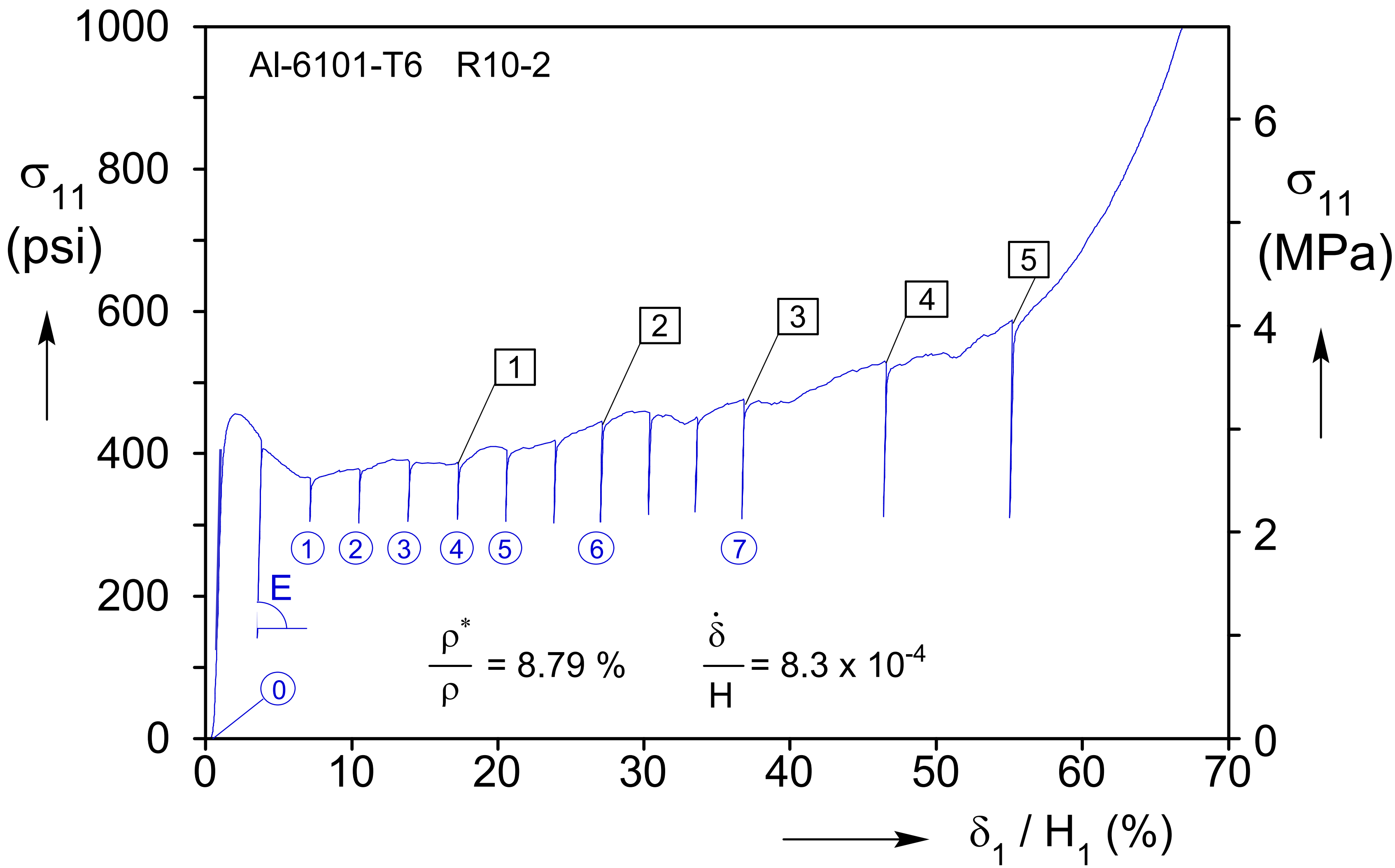

Monitor Deformation at Sites A and B

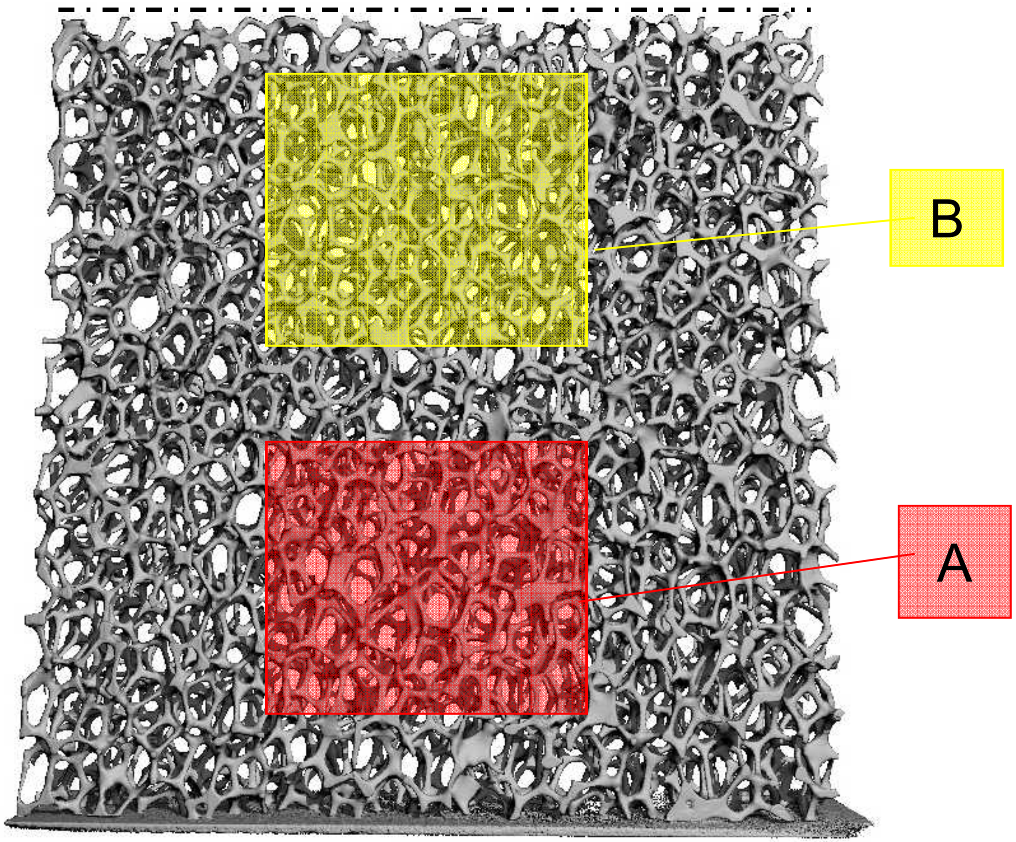

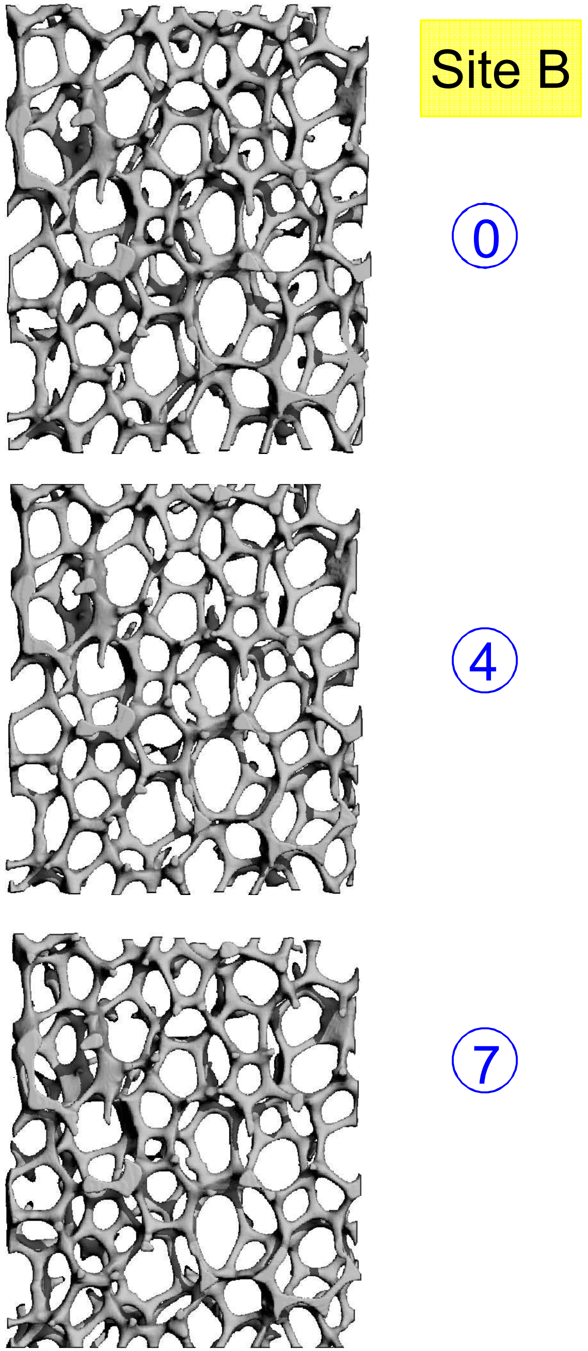

Site A

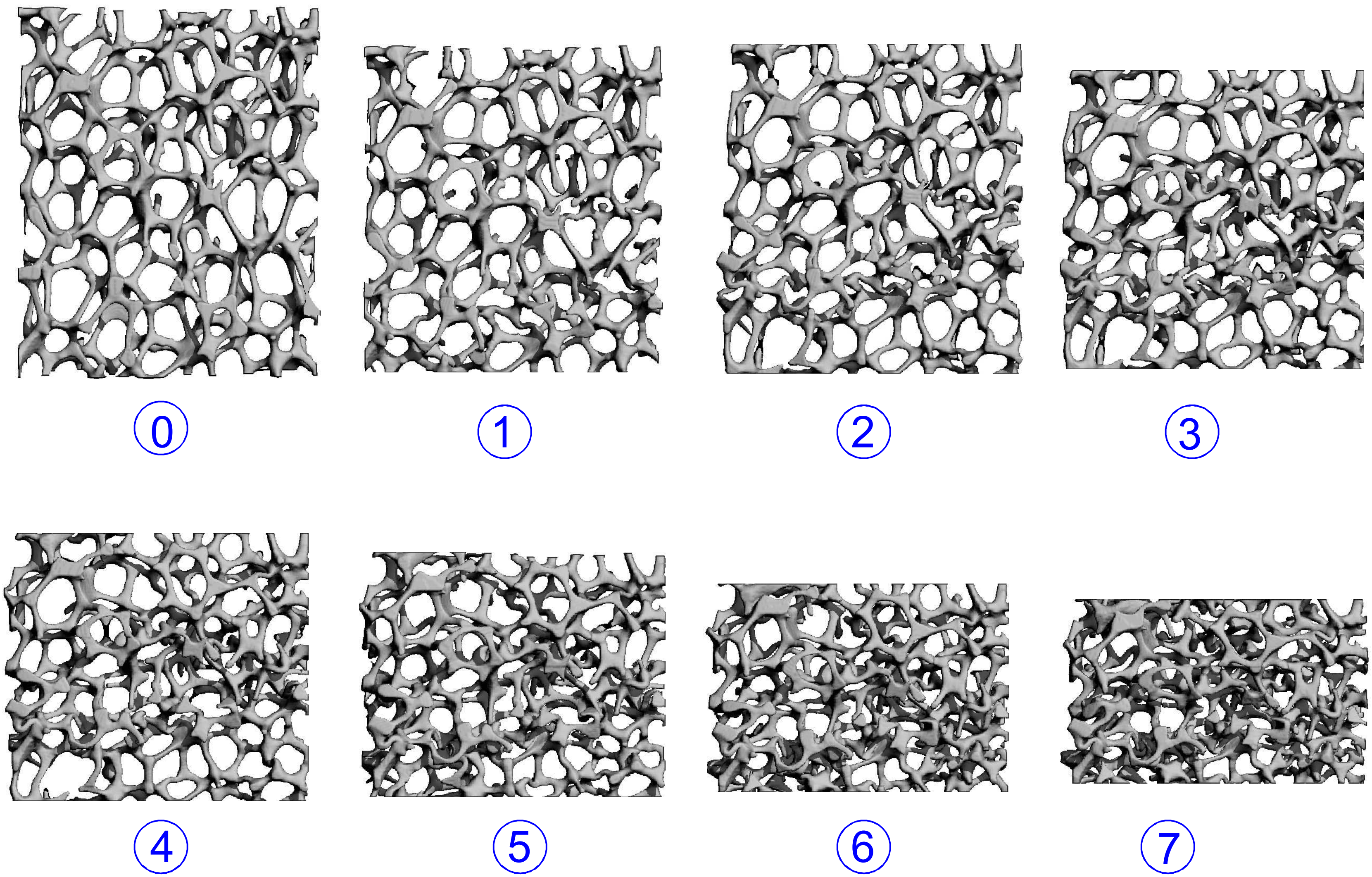

Internal X-Ray Tomography Images of Evolution of Crushing

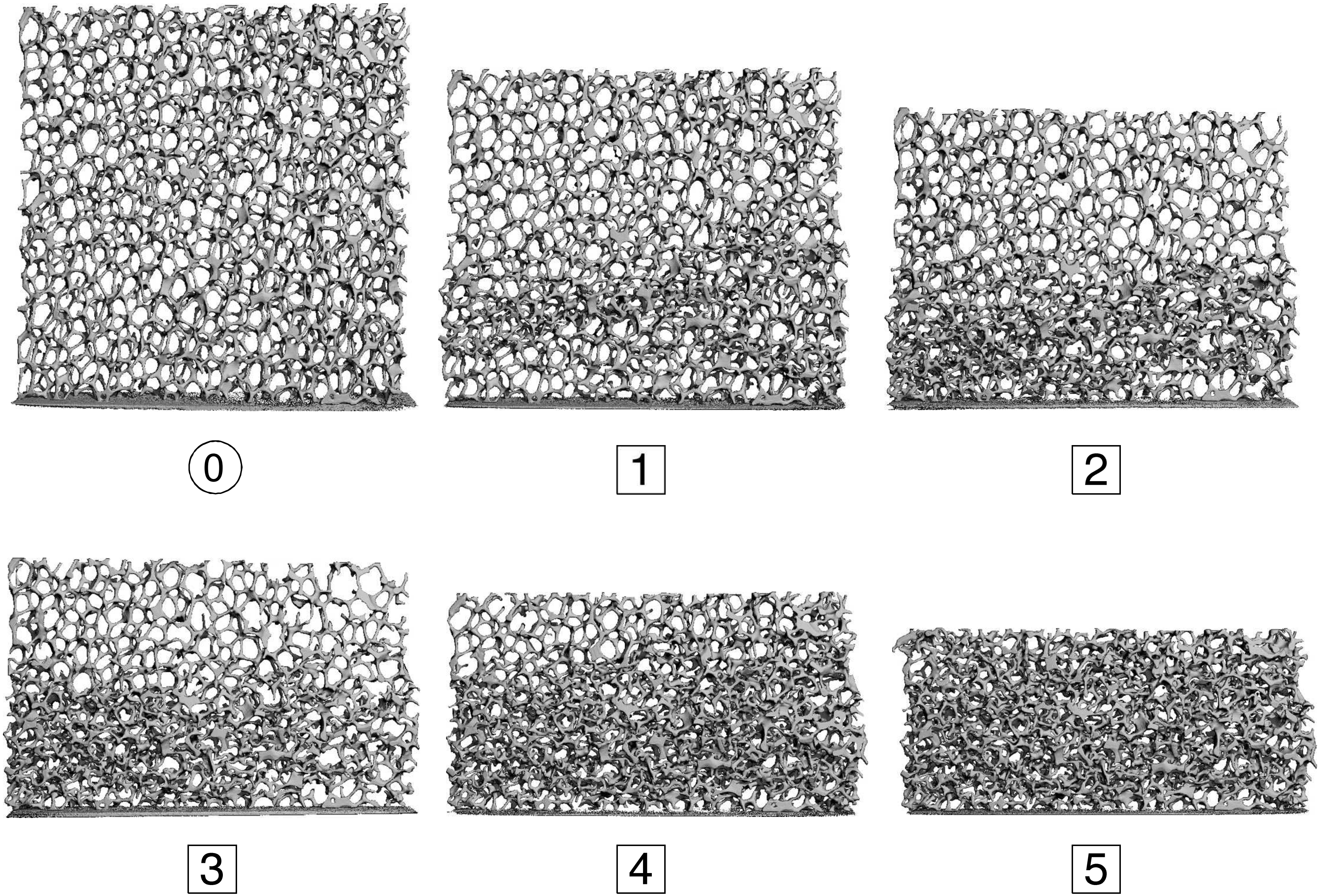

Crushing Responses of Different Cell Size Al Foams

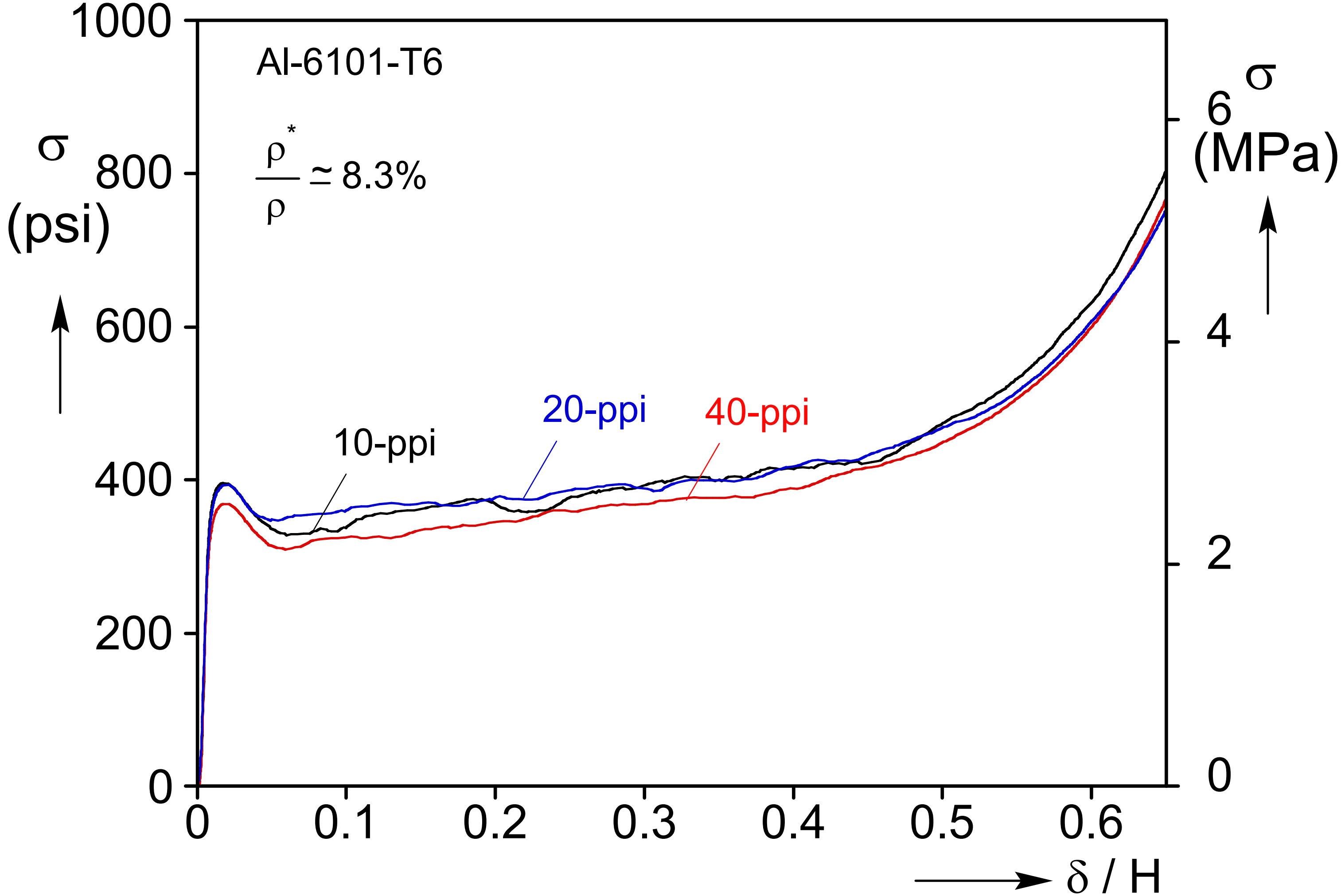

Comparison of Rise and Transverse Responses

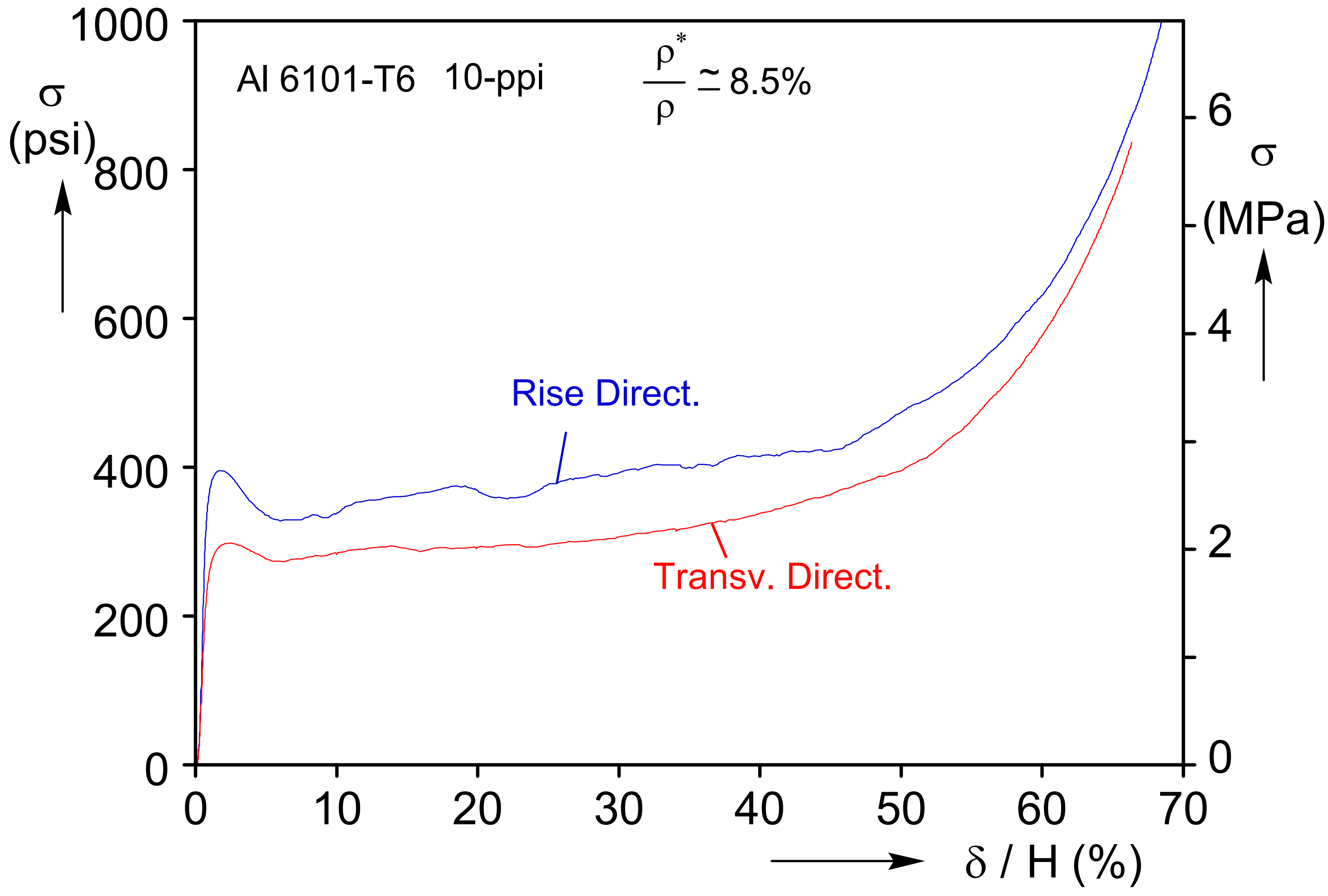

Models for Initial Elastic Moduli

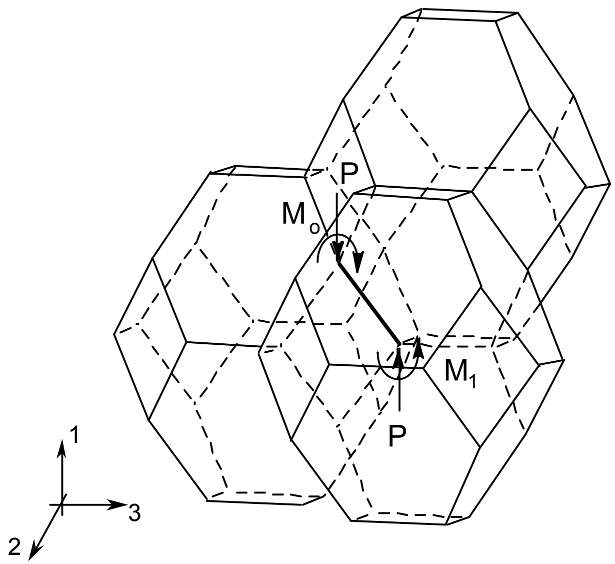

E_{11}

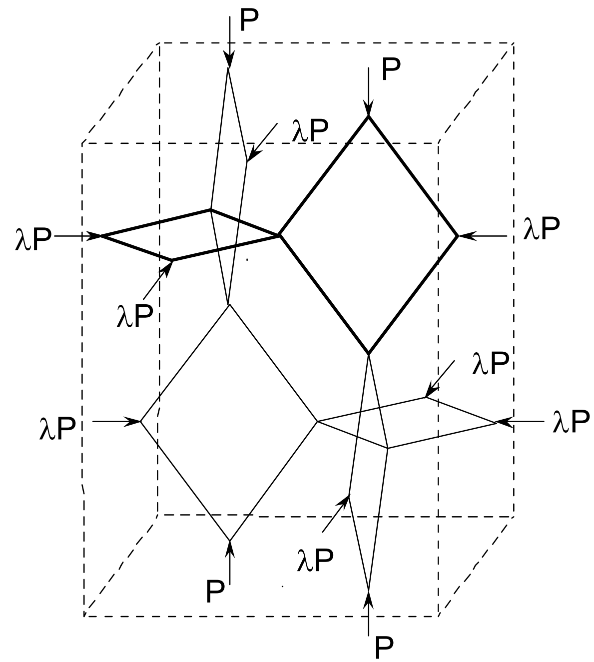

κ

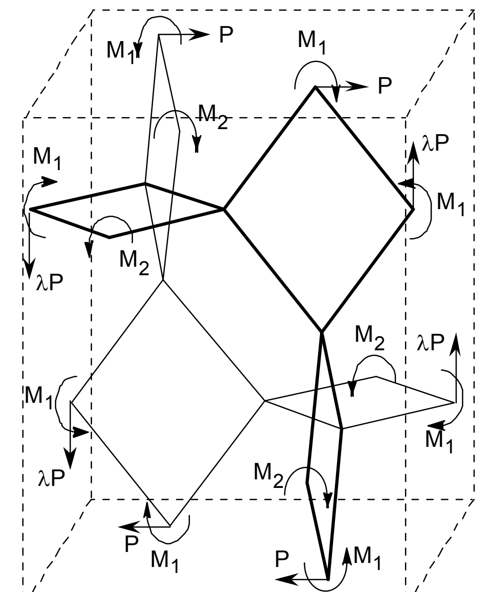

G_{13}

Elastic Moduli

Anisotropic, Nonuniform Cross Section

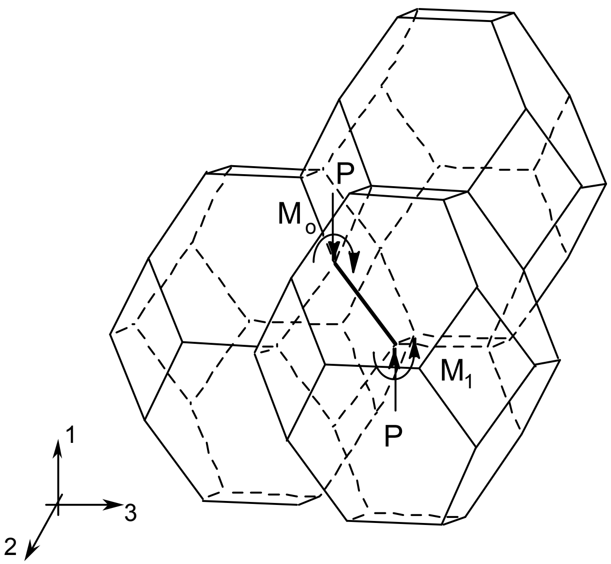

E_1^*

Gong et al., 2005

$\dfrac{\rho^*}{\rho}$	$k\ \bar{r}^n$
$\dfrac{E_1^*}{E}$	$\dfrac{C_I C_A^2 \sin\alpha\ \bar{r}^4}{C_1 + 2C_I C_A C_2 \sin^2\alpha\ \bar{r}^2}$
$\dfrac{E_2^*}{E}, \dfrac{E_3^*}{E}$	$\dfrac{2C_I C_A^2 \cos\alpha\ \bar{r}^4}{\lambda\left[C_1(\lambda^2 + \sqrt{2}\cos\alpha) + C_I C_A C_2 (2\cos^2\alpha + \sqrt{2}\cos\alpha)\ \bar{r}^2\right]}$
ν_{12}^*	$\dfrac{\lambda^2}{2}\left(\dfrac{C_1 - 2C_I C_A C_2 \cos^2\alpha\ \bar{r}^2}{C_1 + 2C_I C_A C_2 \sin^2\alpha\ \bar{r}^2}\right)$
ν_{21}^*	$\dfrac{C_1 - 2C_I C_A C_2 \cos^2\alpha\ \bar{r}^2}{C_1(\lambda^2 + \sqrt{2}\cos\alpha) + (2\cos^2\alpha + \sqrt{2}\cos\alpha) C_I C_A C_2\ \bar{r}^2}$
ν_{23}^*	$\dfrac{C_1 - C_I C_A C_2\ \bar{r}^2}{C_1\left(1 + \dfrac{\lambda^2}{\sqrt{2}\cos\alpha}\right) + (\sqrt{2}\cos\alpha + 1) C_I C_A C_2\ \bar{r}^2}$
$\dfrac{\kappa^*}{E}$	$\dfrac{C_I C_A^2\ \bar{r}^4}{\dfrac{\cos^2 2\alpha}{\sin\alpha\cos^4\alpha} C_1 + (8\sin\alpha + 2\sqrt{2}\lambda) C_I C_A C_2\ \bar{r}^2}$
$\dfrac{G_{12}^*}{E}, \dfrac{G_{13}^*}{E}$	$\dfrac{2\sin\alpha\cos^2\alpha\, C_I C_A^2\ \bar{r}^4}{D_1 + 2\sqrt{2} D_2 \sin^2\alpha\cos\alpha + 2C_I C_A C_2\ \bar{r}^2}$
$\dfrac{G_{23}^*}{E}$	$\dfrac{\cos^3\alpha\, C_I C_A^2\ \bar{r}^4}{\lambda(D_3 + 2\sqrt{2}\cos^3\alpha\, C_I C_A C_2\ \bar{r}^2)}$

Kelvin Characteristic Cell Model

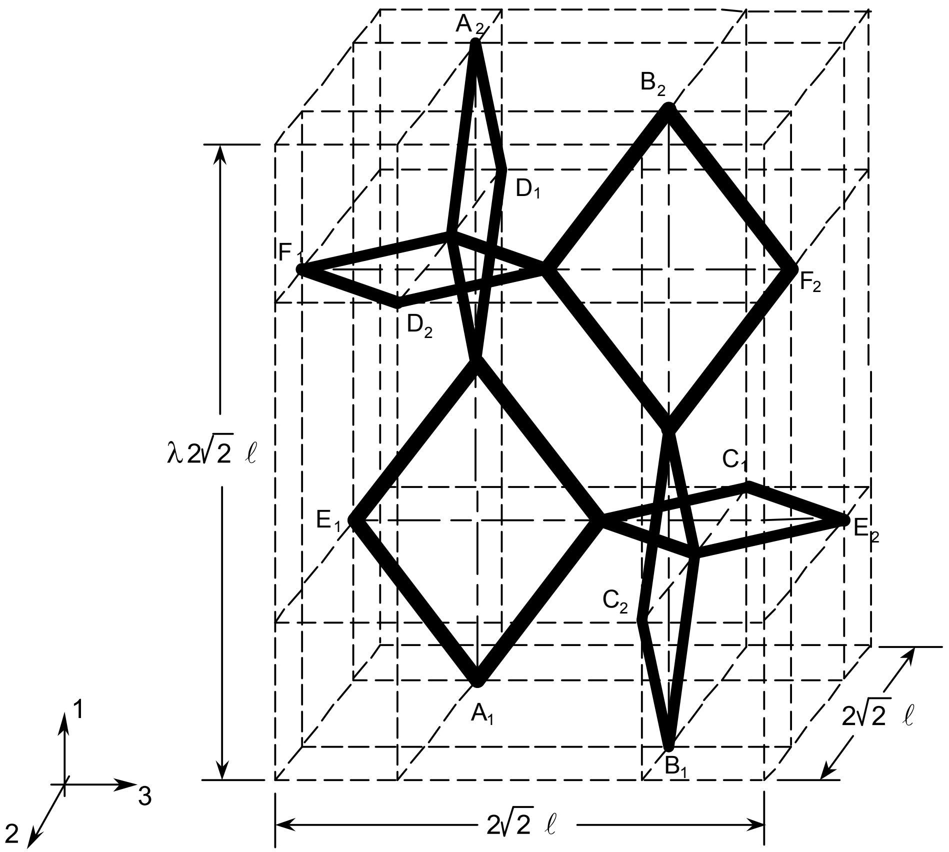

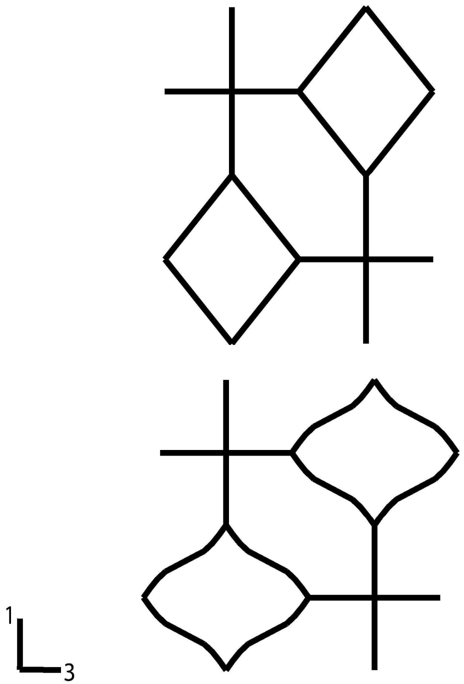

- Beam Element B32
- 192 Elements
- 2268 DOF

* Shear Deformable
* Quadratic - 3 Nodes
* 6 DOF / Node
* 8 Elements / Ligament